International Journal of Non–Linear Mechanics 174 (2025) 105089

Contents lists available at ScienceDirect

International Journal of Non-Linear Mechanics

journal homepage: www.elsevier.com/locate/nlm

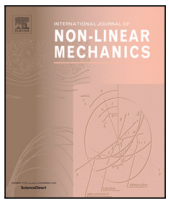

An asymptotic model of vibroadhesion

I. Argatov [a,b], A. Papangelo [c,d], M. Ciavarella [e,d,*]

[a] College of Aerospace Engineering, Chongqing University, Chongqing, 400030, China
[b] Institut für Mechanik, Technische Universität Berlin, 10623 Berlin, Germany
[c] TriboDynamics Lab, Department of Mechanics Mathematics and Management, Politecnico di Bari, via Orabona 4, 70126 Bari, Italy
[d] Department of Mechanical Engineering, Hamburg University of Technology, Am Schwarzenberg-Campus 1, 21073 Hamburg, Germany
[e] Department of Mechanics Mathematics and Management, Politecnico di Bari, Via Orabona 4, Bari, 70125, Italy

ARTICLE INFO

Keywords:
Vibroadhesion
Hysteretic systems
Rate-dependent adhesion
JKR-type adhesion
Nonlinear vibrations
Bogoliubov's averaging
Method of harmonic balance
Asymptotic model

ABSTRACT

A compliantly fixed hemispherical indenter in adhesive contact with an elastic sample firmly bonded to a rigid base is considered under the assumption that the rigid base undergoes small-amplitude high-frequency normal (vertical) oscillations. A general law of the rate-dependent JKR-type adhesion is assumed, which relates the work of adhesion to the contact front velocity. Using the Bogoliubov averaging approach in combination with the method of harmonic balance, the leading-order asymptotic model is constructed for steady-state vibrations. The effective work of adhesion is evaluated in implicit form. A quasi-static approximation for the pull-off force is derived. The case of rigid fixation of the indenter is considered in detail.

1. Introduction

Adhesion as a mechanical phenomenon [1,2] manifests itself in the existence of a non-zero pull-off force which is needed to separate two solids brought into contact [3,4]. As an interface effect [5,6], adhesion strongly depends on the physico-chemical properties of the contacting surfaces as well as — but in a less degree — on the mechanical properties of subsurface layers [7], topography of contact surfaces [8,9], and contact geometry [10,11]. Usually, the adhesion is characterized by the surface energy density, $\Delta\gamma$, measured in joules per meter squared. Even so, the phenomenon of rate-dependent adhesion [12,13], when (in contradiction with the assumption that $\Delta\gamma$ is a constant) the pull-off force markedly depends on the unloading rate [14,15], has been theoretically studied for decades [16–18].

The phenomenological approach to modeling the rate-dependent effects of adhesion in axisymmetric contacts relates the work of adhesion, w, to the contact front velocity, $\dot{a} = \mathrm{d}a/\mathrm{t}$, where a is the contact radius. Since the process of decreasing of the contact area in separating the contacting solids strongly resembles the process of the annular crack propagation along the interface between dissimilar materials (indenter and sample), the mathematical approach of the fracture mechanics was successfully applied [19–21] to associate the law of rate-dependent adhesion with the bulk viscoelasticity of subsurface layers. To date, there is a lack of experimental evidence supporting the developed constitutive models of rate-dependent adhesion [22,23], which prompted the introduction of an *ad hoc* modeling approach [24] for extracting the w vs. $\dot{a}$ relation from experimental data.

In recent years, there has been a growing interest in exploiting the effect of mechanical vibrations to enhance and control the strength of adhesive contacts [25], which can find diverse applications in soft robotics [26,27] and micro-manipulation engineering applications [28]. The mechanism behind this effect is more or less understood [16]: external high-frequency mechanical vibrations (with some angular frequency ω) cause variations in the contact radius a with the same frequency, which happen with the contact front velocity $\dot{a}$ being proportional to ω. This means that the contact front can move (periodically) very fast, thereby activating the adhesion strengthening due to its rate-dependency.

However, despite the known phenomenological mechanism and a wealth of experimental evidence that supports it, no comprehensive mathematical model of vibroadhesion has been proposed in the literature so far. Here we make use of the term 'vibroadhesion' in analogy with the terms 'electroadhesion' [29–31], 'vibrorheology' [32], and 'vibrational mechanics' [33] that investigates the effect of vibrations on friction. The aim of the present paper is to lay a cornerstone in the theoretical foundation of vibroadhesion, which is still in its infancy, despite recent modeling attempts [25,34,35]. It should be noted (see Remark 1 for details) that the previous studies [25,35] numerically investigated a *per se* different dynamic model. However, the main distinction of our

* Corresponding author at: Department of Mechanics Mathematics and Management, Politecnico di Bari, Via Orabona 4, Bari, 70125, Italy.
E-mail address: mciava@poliba.it (M. Ciavarella).

https://doi.org/10.1016/j.ijnonlinmec.2025.105089
Received 28 October 2024; Received in revised form 27 January 2025; Accepted 29 January 2025
Available online 23 March 2025

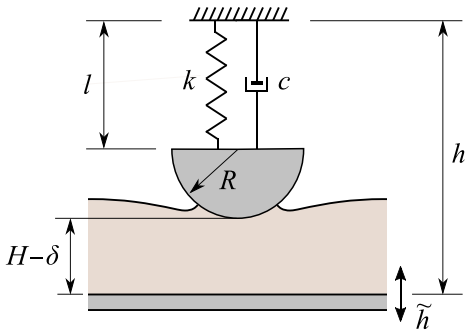

Fig. 1. Schematic of the adhesive contact between a hemispherical probe and an elastic sample: Dynamic equilibrium.

study lies in the application of asymptotic modeling methodology for both quantitative and qualitative analyses of vibroadhesion.

Observe that the Hertzian contact (e.g., between a rigid indenter and an elastic substrate) in dynamic loading can be modeled as a nonlinear oscillator [36,37]. The loaded adhesive compliant contact again can be regarded as a nonlinear oscillator, provided the indenter and the substrate do not lose contact. In the case of rate-dependent adhesion, the contact stiffness in loading (increasing contact) and unloading (decreasing contact) takes different values, and therefore, the rate-dependent adhesive contact exhibits hysteretic behavior [38,39]. However, in contrast to the hysteretic model of localized frictional contacts [40], the force–displacement relations (for loading and unloading) are given in a parametric form in terms of the contact radius a, which plays a role of internal variable, with the contact stiffness being dependent on the time derivative $\dot{a}$.

The rest of the paper is organized as follows. In Section 2.1, we formulate a one-degree-of-freedom dynamic model of instrumented vibrational adhesive indentation testing. In Section 2.2, we solve the problem of steady-state vibrations, using a combination of Bogoliubov's averaging and the method of harmonic balance. The results of our leading-order asymptotic analysis are summarized in Section 3.1. A simple quasi-static estimate for the pull-off force, representing a practically significant result, is derived in Section 3.2. The asymptotic model's predictions are illustrated in Section 3.5 in the case of so-called nominal point contact. The refined asymptotic model, which accounts for the effect of rigid-base excitation frequency, is presented in Section 3.6. Finally, in Section 3.7, we introduce the dynamic contact stiffness and investigate its properties in the special case of rigid fixation of the indenter. The paper is finished with a discussion of the limitations of the constructed asymptotic approximations (including their possible generalizations) and our conclusions.

2. Theory

2.1. Mathematical model of instrumented vibroadhesive indentation

2.1.1. Dynamic equilibrium

We consider normal indentation of an elastic sample of finite thickness, H, performed with a hemispherical indenter of radius, R, and mass, m, and model our mechanical system (see Fig. 1) as a single-degree-of-freedom dynamic system. The total length of the assembly, h, and the length of the fixation element, l, can be represented as follows (compare with Eqs. (A.1) and (A.2) corresponding to the case of static equilibrium):

$$h = l + R + H - \delta, \qquad l = \hat{l} + x_{\mathrm{s}}, \tag{1}$$

where h, l, δ, and x_{s} are now regarded as functions of the time variable, t, and $\hat{l}$ is the length of the fixation element in the unloaded state.

Further, the fixation-element reaction equation is assumed in the form

$$F = kx_{\mathrm{s}} + c\dot{x}_{\mathrm{s}}. \tag{2}$$

Here, k is the stiffness element, c is the damping coefficient, and an over-dot denotes differentiation with respect to t.

According to Newton's second law, the equation of dynamic equilibrium of the indenter takes the form

$$m\ddot{x}_{\mathrm{s}} = mg - P - F, \tag{3}$$

where P is the contact force, and F is given by (2).

Following [13], the JKR model (A.4), (A.5) can be generalized as

$$P = \frac{4E^*a^3}{3R} - \sqrt{8\pi w E^* a^3}, \tag{4}$$

$$\delta = \frac{a^2}{R} - \sqrt{\frac{2\pi w a}{E^*}} \tag{5}$$

by assuming that the work of adhesion w is a function of the contact front velocity $\dot{a}$.

Without specifying the law of rate-dependent adhesion we put

$$w = w_0 f\Big(\frac{\dot{a}}{v_0}\Big), \tag{6}$$

where v_0 is some characteristic velocity, and $f(x)$ is a dimensionless positive (generally speaking, non-negative) function, such that $f(x) > 1$ for $x < 0$ (when the contact decreases) and $f(x) < 1$ for $x > 0$ (when the contact increases). Provided that $f(0) = 1$, Eq. (6) also covers the case of quasi-static loading.

From Eqs. (1), it follows that

$$x_{\mathrm{s}} = h - \hat{h} + \delta, \tag{7}$$

where $\hat{h} = \hat{l} + R + H$ is the total length of the disassembled system elements.

Then, the substitution of the fixation-element reaction (2) into Eq. (3), in view of (7), yields

$$m\ddot{\delta} + c\dot{\delta} + k\delta + P = mg + \mathscr{F}, \tag{8}$$

where $\mathscr{F}$ is the forcing term, defined as

$$\mathscr{F} = -m\ddot{h} - c\dot{h} - k(h - \hat{h}). \tag{9}$$

Thus, the problem of dynamic equilibrium is formed by three Eqs. (4), (5), and (8) with respect to the unknown variables a, P, and δ, provided the total length h is specified as a function of time.

As it concerns the initial conditions that should be specified for the uniqueness of the solution of the second-order differential Eq. (8), the most practically realistic scenario is to start from the position of static equilibrium, that is

$$P|_{t=0} = P_0, \quad \delta|_{t=0} = \delta_0, \quad a|_{t=0} = a_0, \tag{10}$$

where the triple a_0, P_0, and δ_0 solves the static equilibrium problem (A.4), (A.5), and (A.7). It should be also noted here that in the case $\delta \equiv \mathrm{const}$ and $h \equiv \mathrm{const}$, Eq. (8) reduces to Eq. (A.7).

2.2. Steady-state vibroadhesion

We consider the special case when the sample's base is stimulated according to the simple harmonic law

$$h = h_0 + h_1 \sin \omega t, \tag{11}$$

where the displacement amplitude h_1 is supposed to be relatively small, i.e., $h_1 \ll h_0$, so that the indenter does not lose contact with the sample's surface.

It is clear that Eq. (11) is in agreement with the initial conditions (10). But our focus will be on the steady state that is supposed to

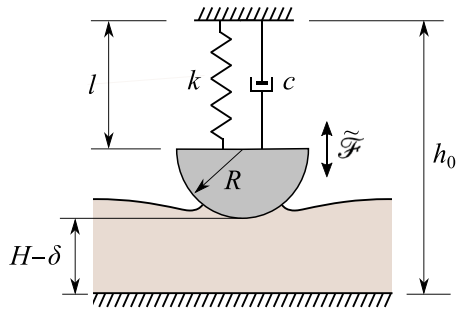

Fig. 2. Schematic of the adhesive contact between a hemispherical probe and an elastic sample: Force excitation.

be established after some initial period. In other words, we are looking for an approximate solution in the form

$$a = a_{\mathrm{m}} + \tilde{a}, \quad P = P_{\mathrm{m}} + \tilde{P}, \quad \delta = \delta_{\mathrm{m}} + \tilde{\delta}, \tag{12}$$

where a_{m}, P_{m}, and δ_{m} are some constant mean values, and $\tilde{a}$, $\tilde{P}$, and $\tilde{\delta}$ are periodic functions of time with the period $2\pi/\omega$ and zero means.

Based on the experimental evidence [22,25], it is anticipated that $a_{\mathrm{m}} > a_0$, and the increase in contact area is a manifestation of the strengthening of adhesion due to the effect of vibrations. The difference $a_{\mathrm{m}} - a_0$ is governed by the two parameters ω and h_1. Our aim here is to establish this relationship, assuming that $|\tilde{a}| \ll a_{\mathrm{m}}$, etc.

Remark 1. It should be noted that in the previous studies [25,35], a *per se* different dynamic model was investigated, which in our notation can be represented as

$$m\ddot{\delta} + c\dot{\delta} + k\delta + P = \mathscr{F}_0 + \tilde{\mathscr{F}}, \tag{13}$$

where $\mathscr{F}_0 = mg - k(h_0 - \hat{h})$ is a static preload, and $\tilde{\mathscr{F}} = \mathscr{F}_1 \sin\omega t$ is the imposed vibrational loading.

The corresponding mechanical scheme is shown in Fig. 2 (compare with Fig. 1). While Eqs. (8) and (13) formally agree with each other, still there are certain nuances in the behaviors of the two dynamic systems, which will be discussed later (see Appendix A).

2.2.1. Application of Bogoliubov's averaging approach

We apply the Bogoliubov averaging approach [41] (see also [42,43]) and introduce the averaging operator

$$\underset{t}{M}\{u(t)\} = \frac{\omega}{2\pi}\int_{-\pi/\omega}^{\pi/\omega} u(t)\,\mathrm{d}t \tag{14}$$

which acts on any integrable $2\pi/\omega$-periodic function $u(t)$.

By the construction of the asymptotic Ansatz (12), we have $\underset{t}{M}\{\tilde{a}\} = 0$, etc. Hence, the application of the Bogoliubov averaging to the differential Eq. (8), in view of (11) and (12), yields the following linear algebraic equation (cf. Eq. (A.7)):

$$h_0 = \hat{h} + \frac{mg}{k} - \frac{P_{\mathrm{m}}}{k} - \delta_{\mathrm{m}}. \tag{15}$$

By neglecting small terms of the second order, we can state that $a^n \simeq a_{\mathrm{m}}^n + n a_{\mathrm{m}}^{n-1}\tilde{a}$, and therefore, $\underset{t}{M}\{a^n\} \simeq a_{\mathrm{m}}^n$. The latter formula can be used for averaging the first terms on the right-hand sides of Eqs. (4) and (5). As it concerns the second terms, we note that $\sqrt{w a^n} \simeq \sqrt{w a_{\mathrm{m}}^n}\big(1 + (n/2)(\tilde{a}/a_{\mathrm{m}})\big)$. Hence, in the leading asymptotic terms we obtain $\sqrt{w a^n} \simeq \sqrt{w a_{\mathrm{m}}^n}$.

Thus, under the smallness assumptions formulated above, the application of the Bogoliubov averaging operator $\underset{t}{M}$ to Eqs. (4) and (5) leads to the following results:

$$P_{\mathrm{m}} = \frac{4E^* a_{\mathrm{m}}^3}{3R} - \sqrt{8\pi w_{\mathrm{eff}} E^* a_{\mathrm{m}}^3}, \tag{16}$$

$$\delta_{\mathrm{m}} = \frac{a_{\mathrm{m}}^2}{R} - \sqrt{\frac{2\pi w_{\mathrm{eff}} a_{\mathrm{m}}}{E^*}}. \tag{17}$$

Here, w_{eff} is the effective work of adhesion defined by the relation

$$\sqrt{w_{\mathrm{eff}}} = \underset{t}{M}\{\sqrt{w}\}. \tag{18}$$

In view of $(12)_1$, (14), and (6), Eq. (18) can be rewritten as

$$w_{\mathrm{eff}} = w_0\left(\frac{\omega}{2\pi}\int_{-\pi/\omega}^{\pi/\omega}\sqrt{f\Big(\frac{1}{v_0}\frac{\mathrm{d}\tilde{a}}{\mathrm{d}t}\Big)}\,\mathrm{d}t\right)^2. \tag{19}$$

Observe that Eqs. (16) and (17) exactly preserve the structure of the JKR model. The only essential difference is that the steady-state solution is strictly related to the oscillatory part of the solution (which is determined by the second terms on the right-hand sides of Eqs. (12)) by means of the effective work of adhesion (19).

2.2.2. Application of the method of harmonic balance

The effective work of adhesion w_{eff} determines the steady state (solution to the averaged model (16) and (17)), but right-hand side of Eq. (19) depends on the oscillatory part $\tilde{a}$. Hence, the original problem requires further study, and to do this we apply the method of harmonic balance, which can be regarded as a Galerkin procedure [44] and is known [45] to be originally founded on the work of Krylov and Bogoliubov [46].

The substitution of $(12)_2$ and $(12)_3$ into Eq. (8), in view of (15), yields

$$m\ddot{\tilde{\delta}} + c\dot{\tilde{\delta}} + k\tilde{\delta} + \tilde{P} = \tilde{\mathscr{F}}, \tag{20}$$

where we have introduced the notation

$$\tilde{\mathscr{F}} = -m\ddot{\tilde{h}} - c\dot{\tilde{h}} - k\tilde{h}, \qquad \tilde{h} = h - h_0. \tag{21}$$

In view of (11), we have $\tilde{h} = h_1 \sin\omega t$ and

$$\tilde{\mathscr{F}} = -h_1\left[(k - m\omega^2)\sin\omega t + c\omega\cos\omega t\right]. \tag{22}$$

Further, by taking into account Eqs. (12), (16), and (17), the adhesion submodel (4) and (5) can be linearized with respect to the contact radius perturbation $\tilde{a}$ as follows:

$$\tilde{P} \simeq \left(\frac{4E^*}{R}a_{\mathrm{m}}^2 - 3\sqrt{2\pi w E^* a_{\mathrm{m}}}\right)\tilde{a} + \sqrt{8\pi E^* a_{\mathrm{m}}^3}\left(\sqrt{w_{\mathrm{eff}}} - \sqrt{w}\right), \tag{23}$$

$$\tilde{\delta} \simeq \left(\frac{2a_{\mathrm{m}}}{R} - \sqrt{\frac{\pi w}{2E^* a_{\mathrm{m}}}}\right)\tilde{a} + \sqrt{\frac{2\pi a_{\mathrm{m}}}{E^*}}\left(\sqrt{w_{\mathrm{eff}}} - \sqrt{w}\right). \tag{24}$$

To efficiently construct the leading asymptotic terms, we assume that

$$\tilde{a} = A\sin\omega t', \qquad t' = t + \frac{\varphi}{\omega}, \tag{25}$$

where A and φ are the amplitude and phase of the contact radius variation.

Then, the substitution of $(25)_1$ into Eq. (6) yields the approximation

$$w = w_0 f\Big(\frac{A\omega}{v_0}\cos\omega t'\Big), \tag{26}$$

so that the following Fourier expansion holds:

$$\sqrt{f(\bar{A}\cos\omega t')} = \mathscr{J}_0(\bar{A}) + \mathscr{J}_{c1}(\bar{A})\cos\omega t' \ldots. \tag{27}$$

Here we have introduced the notation ($n = 1, 2, \ldots$)

$$\mathscr{J}_0(\bar{A}) = \frac{1}{\pi}\int_0^{\pi}\sqrt{f(\bar{A}\cos x)}\,\mathrm{d}x, \tag{28}$$

$$\mathscr{J}_{cn}(\bar{A}) = \frac{2}{\pi}\int_0^{\pi}\sqrt{f(\bar{A}\cos x)}\cos nx\,\mathrm{d}x. \tag{29}$$

It should be noted that the function on the left-hand side of Eq. (27) is an even function of the variable t', and therefore, its sine Fourier coefficients vanish. This happened due to the local time transformation $(25)_2$. From Eqs. (25)–(29), it follows that in their leading asymptotic terms the contact variation variables $\tilde{a}$, $\tilde{P}$, and $\tilde{\delta}$ are not in phase.

Let us introduce the short-hand notation

$$\left\{ \begin{matrix} \tilde{\delta}_{\mathrm{c}} \\ \tilde{\delta}_{\mathrm{s}} \end{matrix} \right\} = \frac{\omega}{\pi} \int_{-\pi/\omega}^{\pi/\omega} \left\{ \begin{matrix} \cos \omega t' \\ \sin \omega t' \end{matrix} \right\} \tilde{\delta} \, \mathrm{d}t', \tag{30}$$

$$\left\{ \begin{matrix} \tilde{P}_{\mathrm{c}} \\ \tilde{P}_{\mathrm{s}} \end{matrix} \right\} = \frac{\omega}{\pi} \int_{-\pi/\omega}^{\pi/\omega} \left\{ \begin{matrix} \cos \omega t' \\ \sin \omega t' \end{matrix} \right\} \tilde{P} \, \mathrm{d}t'. \tag{31}$$

Then, the harmonic balance of Eqs. (23) and (24), respectively, implies that

$$\tilde{P}_{\mathrm{s}} = \left\{ \frac{4E^*}{R} a_{\mathrm{m}}^2 - 3\sqrt{2\pi w_0 E^* a_{\mathrm{m}}} \, \mathcal{J}_1\Big(\frac{\omega A}{v_0}\Big) \right\} A, \tag{32}$$

$$\tilde{\delta}_{\mathrm{s}} = \left\{ \frac{2a_{\mathrm{m}}}{R} - \sqrt{\frac{\pi w_0}{2E^* a_{\mathrm{m}}}} \, \mathcal{J}_1\Big(\frac{\omega A}{v_0}\Big) \right\} A, \tag{33}$$

$$\tilde{P}_{\mathrm{c}} = -\sqrt{8\pi E^* w_0 a_{\mathrm{m}}^3} \, \mathcal{J}_{\mathrm{c1}}\Big(\frac{\omega A}{v_0}\Big), \tag{34}$$

$$\tilde{\delta}_{\mathrm{c}} = -\sqrt{\frac{2\pi w_0 a_{\mathrm{m}}}{E^*}} \, \mathcal{J}_{\mathrm{c1}}\Big(\frac{\omega A}{v_0}\Big), \tag{35}$$

where we have introduced the notation

$$\mathcal{J}_1(\bar{A}) = \frac{2}{\pi} \int_0^{\pi} \sqrt{f(\bar{A}\cos x)} \sin^2 x \, \mathrm{d}x. \tag{36}$$

Now, returning to the differential Eq. (20), we make the change of the time variable $(25)_2$ and rewrite that equation in the form

$$m\tilde{\delta}'' + c\tilde{\delta}' + k\tilde{\delta} + \tilde{P} = \tilde{\mathcal{F}}, \tag{37}$$

where the prime denotes the differentiation with respect to t' and, in view of (22), we have

$$\begin{aligned} \tilde{\mathcal{F}} \; = \; & -h_1 \, \big\{ \, [(k - m\omega^2)\cos\varphi + c\omega \sin\varphi] \sin \omega t' \\ & + [c\omega \cos\varphi - (k - m\omega^2)\sin\varphi] \cos \omega t' \, \big\} \, . \end{aligned} \tag{38}$$

By subsequently multiplying both sides of Eq. (37) by $\cos \omega t'$ and $\sin \omega t'$ and integrating over the period we obtain

$$-h_1[c\omega \cos\varphi - (k - m\omega^2)\sin\varphi] = \Xi_{\mathrm{c}}, \tag{39}$$

$$-h_1[(k - m\omega^2)\cos\varphi + c\omega \sin\varphi] = \Xi_{\mathrm{s}}, \tag{40}$$

where we have introduced the short-hand notation

$$\Xi_{\mathrm{c}} = (k - m\omega^2)\tilde{\delta}_{\mathrm{c}} + c\omega\tilde{\delta}_{\mathrm{s}} + \tilde{P}_{\mathrm{c}}, \tag{41}$$

$$\Xi_{\mathrm{s}} = (k - m\omega^2)\tilde{\delta}_{\mathrm{s}} - c\omega\tilde{\delta}_{\mathrm{c}} + \tilde{P}_{\mathrm{s}}. \tag{42}$$

Now, we can eliminate the unknown variable φ by utilizing the main trigonometric identity $\cos^2\varphi + \sin^2\varphi = 1$, thereby arriving at the equation

$$\Xi_{\mathrm{c}}^2 + \Xi_{\mathrm{s}}^2 = [(k - m\omega^2)^2 + c^2\omega^2]h_1^2, \tag{43}$$

where Ξ_{c} and Ξ_{s} are given by (41) and (42), respectively.

Finally, by taking into account relations (32), (33), (41), and (42), we can transform Eq. (43) into the sought-for relation that relates the amplitude A of the contact radius variation $\tilde{a}$ to the rigid-base excitation parameters h_1 and ω.

Observe that up to this point, we did not *explicitly* employ the assumption of high-frequency oscillations. Now, assuming that $\omega \gg \sqrt{k/m}$, in view of (41) and (42), we can simplify Eq. (43) as follows:

$$|\tilde{\delta}_{\mathrm{c}}| = h_1. \tag{44}$$

The mechanical meaning of Eq. (44) will be discussed later (see Section 3.6 and Appendix B).

3. Results

3.1. Leading-order asymptotic model

Let us introduce the dimensionless contact-radius amplitude

$$\bar{A} = \frac{\omega A}{v_0}, \tag{45}$$

where v_0 is the characteristic velocity that enters the law of rate-dependent adhesion (6). In what follows, the dimensionless variable $\bar{A}$ for simplicity will be called the internal variable.

So, by taking into account Eq. (45), formula (33) can be rewritten as

$$\Big(\frac{E^*}{2\pi w_0 a_{\mathrm{m}}}\Big)^{1/2} \tilde{\delta}_{\mathrm{s}} = \underline{\Big(\frac{2a_{\mathrm{m}}}{R}\sqrt{\frac{E^* R}{\pi w_0}} - \mathcal{J}_1(\bar{A})\Big)\frac{A}{a_{\mathrm{m}}}}. \tag{46}$$

In the spirit of the asymptotic relation (24), the underlined term in the asymptotic formula (46) can be dropped in the limit of negligible contact area variations (when $A \ll a_{\mathrm{m}}$), so that we will have

$$\left\{ \begin{matrix} \tilde{\delta}_{\mathrm{c}} \\ \tilde{\delta}_{\mathrm{s}} \end{matrix} \right\} \simeq -\sqrt{\frac{2\pi w_0 a_{\mathrm{m}}}{E^*}} \left\{ \begin{matrix} \mathcal{J}_{\mathrm{c1}}(\bar{A}) \\ 0 \end{matrix} \right\}. \tag{47}$$

In the same way, the asymptotic formulas (32) and (34) can be simplified as

$$\left\{ \begin{matrix} \tilde{P}_{\mathrm{c}} \\ \tilde{P}_{\mathrm{s}} \end{matrix} \right\} \simeq -\sqrt{8\pi E^* w_0 a_{\mathrm{m}}^3} \left\{ \begin{matrix} \mathcal{J}_{\mathrm{c1}}(\bar{A}) \\ 0 \end{matrix} \right\}. \tag{48}$$

Further, according to Eqs. (19) and (26), the effective work of adhesion can be evaluated as

$$w_{\mathrm{eff}} = w_0[\mathcal{J}_0(\bar{A})]^2, \tag{49}$$

where the integral $\mathcal{J}_0(\bar{A})$ is given by (28). The above formula defines the effective characteristic of vibroadhesion w_{eff} in implicit form, as the internal parameter $\bar{A}$, along with the relative mean contact radius a_{m}, needs to be determined in terms of the rigid-base excitation parameters ω and h_1.

3.1.1. Compliant fixation of the indenter

In view of $(25)_1$, (47), and (48), Eqs. (41) and (42) can be rewritten as follows:

$$\Xi_{\mathrm{c}} = -\sqrt{\frac{2\pi w_0 a_{\mathrm{m}}}{E^*}} \, (k - m\omega^2)\mathcal{J}_{\mathrm{c1}}(\bar{A}) - \sqrt{8\pi E^* w_0 a_{\mathrm{m}}^3} \, \mathcal{J}_{\mathrm{c1}}(\bar{A}), \tag{50}$$

$$\Xi_{\mathrm{s}} = \sqrt{\frac{2\pi w_0 a_{\mathrm{m}}}{E^*}} \, c\omega \mathcal{J}_{\mathrm{c1}}(\bar{A}). \tag{51}$$

Correspondingly, the JKR-type Eqs. (16) and (17) take form

$$P_{\mathrm{m}} = \frac{4E^* a_{\mathrm{m}}^3}{3R} - \sqrt{8\pi w_0 E^* a_{\mathrm{m}}^3} \, \mathcal{J}_0(\bar{A}), \tag{52}$$

$$\delta_{\mathrm{m}} = \frac{a_{\mathrm{m}}^2}{R} - \sqrt{\frac{2\pi w_0 a_{\mathrm{m}}}{E^*}} \, \mathcal{J}_0(\bar{A}). \tag{53}$$

Thus, the substitution of the above expressions for P_{m} and δ_{m} into the averaged balance Eq. (15) yields the relation

$$\begin{aligned} \hat{h} - h_0 + \frac{mg}{k} \; = \; & -\Big(\frac{1}{k}\sqrt{8\pi w_0 E^* a_{\mathrm{m}}^3} + \sqrt{\frac{2\pi w_0 a_{\mathrm{m}}}{E^*}}\Big)\mathcal{J}_0(\bar{A}) \\ & + \frac{4E^* a_{\mathrm{m}}^3}{3Rk} + \frac{a_{\mathrm{m}}^2}{R}, \end{aligned} \tag{54}$$

where the left-hand side is supposed to be known.

To this end, we have got one Eq. (54) for two unknowns a_{m} and $\bar{A}$. The second equation follows from Eq. (43) upon substituting the expressions (50) and (51).

3.1.2. Rigid fixation of the indenter

In the limit as $k/(E^*R)$ goes to infinity, from Eqs. (43), (50), and (51), it follows that

$$|\mathcal{J}_{c1}(\bar{A})| = h_1\sqrt{\frac{E^*}{2\pi w_0 a_m}}. \tag{55}$$

In the same way, Eq. (53) reduces to the equation

$$\frac{a_m^2}{R} - \sqrt{\frac{2\pi w_0 a_m}{E^*}}\,\mathcal{J}_0(\bar{A}) = \hat{h} - h_0. \tag{56}$$

The system of two Eqs. (55) and (56) allows to determine both parameters a_m and $\bar{A}$. After that the mean contact parameters P_m and δ_m can be found from Eqs. (52) and (53).

It should be noted that, in view of (47), Eq. (55) completely agrees with Eq. (44), which was derived in the limit of high frequency oscillations.

3.1.3. Free indenter under the dead weight

Now, by setting $k = c = 0$, Eqs. (51), (43), and (50), respectively, simplify as $\Xi_s = 0$ and

$$|\Xi_c| = m\omega^2 h_1, \tag{57}$$

where

$$\Xi_c = \sqrt{\frac{2\pi w_0 a_m}{E^*}}\,m\omega^2\mathcal{J}_{c1}(\bar{A}) - \sqrt{8\pi E^* w_0 a_m^3}\mathcal{J}_{c1}(\bar{A}). \tag{58}$$

At the same time, in the limit as k goes to zero, Eq. (54) reduces to the relation

$$mg = \frac{4E^* a_m^3}{3R} - \sqrt{8\pi w_0 E^* a_m^3}\,\mathcal{J}_0(\bar{A}), \tag{59}$$

which, in light of Eqs. (16) and (49), simply states that $P_m = mg$.

3.2. Quasi-static estimate for the pull-off force

First of all, we observe that strictly speaking the developed asymptotic model of steady-state vibrations assumes that $a_m = \text{const}$. This, in particular, means that $h_0 = \text{const}$ in the rigid-base excitation law (11). In principle, the steady-state model can be applied outside the range of its applicability for approximate analysis of the effect of a slowly varying modulation $h_0(t)$ of the vibration excitation.

To estimate the vibration effect on the pull-off force, we determine the latter by assuming that the detachment occurs when the mean contact radius a_m reaches the JKR critical value

$$a_{cr} = \left(\frac{9\pi R^2 w_{eff}}{8E^*}\right)^{1/3}, \tag{60}$$

which is evaluated for the corresponding effective work of adhesion.

Thus, in view of (49), we transform Eq. (60) as

$$a_{cr} = \left(\frac{9\pi R^2 w_0}{8E^*}\right)^{1/3}[\mathcal{J}_0(\bar{A}_{cr})]^{2/3}, \tag{61}$$

where the integral $\mathcal{J}_0(\bar{A})$ as a function of $\bar{A}$ is defined by formula (28).

Since we put $a_m = a_{cr}$, Eq. (43) will be the only equation left for evaluation of the corresponding parameter $\bar{A}_{cr}$. In the case under consideration, Eqs. (50) and (51) can be transformed as

$$\frac{\Xi_c}{R} = -\frac{\chi_0^2}{3}\mathcal{J}_0^{1/3}(k - m\omega^2)\mathcal{J}_{c1} - \frac{RE^*}{3}\chi_0^3\mathcal{J}_0\mathcal{J}_{c1}, \tag{62}$$

$$\frac{\Xi_s}{R} = \frac{\chi_0^2}{3}c\omega\mathcal{J}_0^{1/3}\mathcal{J}_{c1}, \tag{63}$$

where the argument $\bar{A}_{cr}$ of the functions $\mathcal{J}_0$ and $\mathcal{J}_{c1}$ has been dropped for the sake of simplicity of notation, and we have introduced the dimensionless parameter

$$\chi_0 = \left(\frac{9\pi w_0}{E^* R}\right)^{1/3}. \tag{64}$$

Further, let us also introduce the notation

$$\omega_0 = \sqrt{\frac{k}{m}}, \quad \zeta = \frac{c}{2\sqrt{km}}, \quad \bar{\omega} = \frac{\omega}{\omega_0}, \quad \eta_1 = \frac{h_1}{R}, \tag{65}$$

$$\kappa = \frac{k}{E^* R}, \tag{66}$$

so that we will have $k - m\omega^2 = k(1 - \bar{\omega}^2)$ and $c/k = 2\zeta/\omega_0$.

Then, Eq. (43) can be non-dimensionalized as

$$\frac{\xi_c^2 + \xi_s^2}{(1 - \bar{\omega}^2)^2 + 4\zeta^2\bar{\omega}^2} = \eta_1^2, \tag{67}$$

where, according to Eqs. (62), (63), and (65), we have

$$\xi_c = \frac{\chi_0^2}{3}\mathcal{J}_0^{1/3}(1 - \bar{\omega}^2)\mathcal{J}_{c1} + \frac{\chi_0^3}{3\kappa}\mathcal{J}_0\mathcal{J}_{c1}, \tag{68}$$

$$\xi_s = -\frac{2\chi_0^2}{3}\zeta\bar{\omega}\mathcal{J}_0^{1/3}\mathcal{J}_{c1}. \tag{69}$$

The substitution of the above expressions into Eq. (67) gives the equation for evaluating the critical value, $\bar{A}_{cr}$, of the internal variable $\bar{A}$. After that, the pull-off force can be estimated by using the JKR result as

$$-P_{cr} = \frac{3\pi}{2}Rw_{eff}, \tag{70}$$

where w_{eff} is the corresponding effective work of adhesion, that is $w_{eff} = w_0[\mathcal{J}_0(\bar{A}_{cr})]^2$ (see Eq. (49)). We recall that by convention the compressive/tensile contact force is assumed to be positive/negative.

The relative effect of vibrations on the pull-off force can be characterized by the ratio

$$\frac{P_{cr}}{P_{cr}^{JKR}} = [\mathcal{J}_0(\bar{A}_{cr})]^2, \tag{71}$$

where $P_{cr}^{JKR} = -(3\pi/2)Rw_0$ is the JKR pull-off force.

3.2.1. Estimate for the pull-off force in the case of rigid fixation

In view of (65), Eq. (55) now takes the form

$$\mathcal{J}_0^{1/3}(\bar{A})|\mathcal{J}_{c1}(\bar{A})| = \frac{3\eta_1}{\chi_0^2}, \tag{72}$$

which determines the critical value $\bar{A}_{cr}$.

From Eq. (72), it follows that the dimensionless parameter $\bar{A}_{cr}$ is a function of the ratio $\eta_1 = h_1/R$. This means that for a given value of the right-hand side of Eq. (72), the predicted value of the relative pull-off force (71) in the leading asymptotic term is independent of ω.

Remark 2. It should be emphasized that in the model under consideration the tested material is assumed to be purely elastic, and the adopted constitutive model (Hooke's law) does not include any bulk material dissipation. However, in the case of vibrational loading, a tested viscoelastic material near the moving contact contour will oscillate with the frequency $\omega/2\pi$, thereby exhibiting the local stiffening effect (see [16] among others). That is why, for a more realistic prediction of the pull-off force, the reduced elastic modulus $E^* = E/(1 - \nu^2)$ in formula (64) should be replaced with $E_1(\omega)/(1 - \nu^2)$, where $E_1(\omega)$ is the storage modulus of the tested viscoelastic material.

3.3. Case of the Gent–Schultz law of rate-dependent adhesion

We consider a very popular empirical model of rate-dependent adhesion introduced by Gent and Schultz [12], which for the case of shrinking contact (opening crack) can be represented as

$$w = w_0\left\{1 + \left(|\dot{a}|/v_0\right)^n\right\}, \tag{73}$$

where $n > 0$ is a fitting parameter, and v_0 is some characteristic crack front velocity. It should be kept in mind [47] that the Gent–Schultz law is applicable only in a certain range of contact-front velocities.

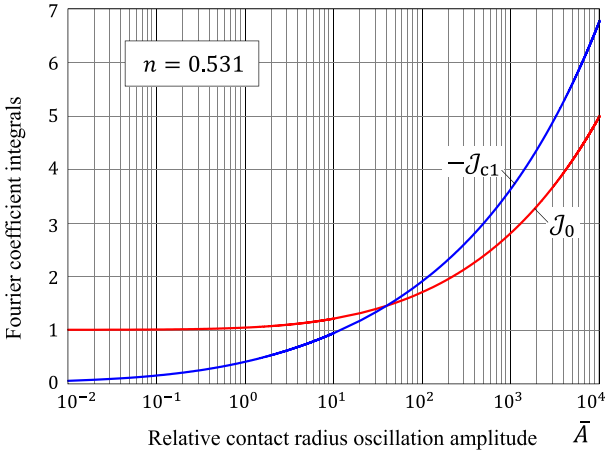

Fig. 3. The Fourier coefficient integrals for the Gent–Schultz model (75).

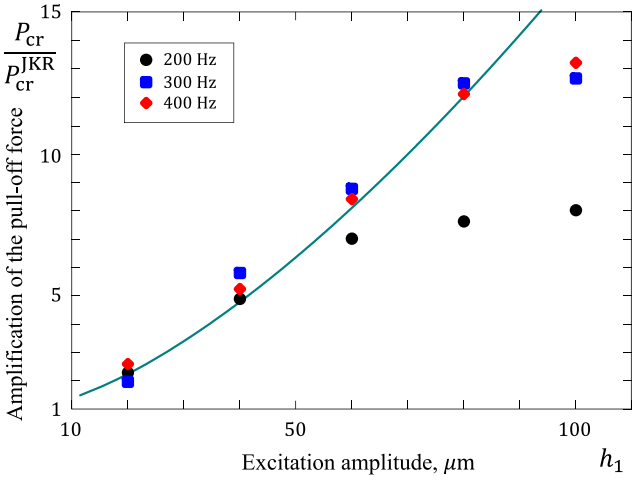

Fig. 4. Vibroadhesive amplification of the pull-off force: The effect of the base excitation amplitude. The experimental data [35,48] was fitted with the leading-order asymptotic model (71), (72) for the Gent–Schultz law with the parameters $w_0 = 0.236\,\mathrm{J/m^2}$, $n = 0.531$, and $v_0 = 44.5$ μm.

In what follows, the right-hand side of Eq. (73) will be denoted by $f_{\mathrm{op}}(|\dot{a}|/v_0)$. For the case of expanding contact (closing crack), the following relation is usually used [25]:

$$f_{\mathrm{cl}}(|\dot{a}|/v_0) = \left[f_{\mathrm{op}}(|\dot{a}|/v_0)\right]^{-1} \tag{74}$$

Thus, in view of (73) and (74), we will have

$$f(\bar{A}\cos x) = \begin{cases} f_{\mathrm{op}}(\bar{A}\cos x), & \cos x < 0, \\ \left[f_{\mathrm{op}}(\bar{A}\cos x)\right]^{-1}, & \cos x > 0. \end{cases} \tag{75}$$

Further, according to the definition of the integral $\mathcal{J}_0(\bar{A})$ (see formula (28)), we have

$$\mathcal{J}_0(\bar{A}) = \frac{1}{\pi}\int_0^{\pi/2} \left\{\sqrt{f_{\mathrm{op}}(\bar{A}\cos x)} + \sqrt{f_{\mathrm{cl}}(\bar{A}\cos x)}\right\} \mathrm{d}x. \tag{76}$$

For the Gent–Schultz model (73)–(75), formula (76) is specified as

$$\mathcal{J}_0(\bar{A}) = \frac{1}{\pi}\int_0^{\pi/2} \left\{\left[1 + (\bar{A}\cos x)^n\right]^{-1/2} + \left[1 + (\bar{A}\cos x)^n\right]^{1/2}\right\} \mathrm{d}x, \tag{77}$$

and similar formulas can be easily derived for $\mathcal{J}_{\mathrm{c}1}(\bar{A})$ and $\mathcal{J}_1(\bar{A})$.

We note, and this can be verified numerically, that the first terms on the right-hand sides of Eqs. (76) and (77) become less important as $\bar{A}$ tends to infinity.

Fig. 3 shows the variation of the integrals $\mathcal{J}_0(\bar{A})$ and $-\mathcal{J}_{\mathrm{c}1}(\bar{A})$ in the case of the Gent–Schultz model. Both functions are monotonic with respect to their argument and grow like $\bar{A}^{n/2}$ as $\bar{A} \to \infty$.

3.4. Fitting experimental data for the pull-off force

We recall that the right-hand side of Eq. (72) is independent of the excitation frequency ω, since the quasi-static approximation for the pull-off force has been derived in the high-frequency oscillation limit.

It is of interest to verify the asymptotic model's predictions against the recent experimental data [35,48] obtained for a polydimethylsiloxane (PDMS) sample with a hemispherical indenter of radius $R = 51.5$ mm. The Gent–Schultz law [12] is used for describing the adhesion's rate-dependency. Based on the experimental data for the storage elastic modulus [23] as a function of the angular frequency in the range $\omega \le 2500\,\mathrm{rad/s}$, the equilibrium elastic modulus $E = 2.8\,\mathrm{MPa}$ has been amplified by the factor of 2. In this special case, we have $\chi_0 = 0.026$. As it is seen from Fig. 4, the fact that the experimental data for the excitation frequencies 300 Hz and 400 Hz do not differ much, supports the asymptotic model's implication drawn above that the pull-off force in the high-frequency vibroadhesion is insensitive to the excitation frequency.

3.5. Nominal point contact

3.5.1. Static nominal point contact

We consider the special case when

$$h_0 = \hat{h}, \tag{78}$$

so that Eq. (A.7) simplifies to

$$\delta_0 + \frac{P_0}{k} = \frac{mg}{k}. \tag{79}$$

For a rigid fixation element, Eq. (79) yields $\delta_0 = 0$, and any nonzero contact area will be established exclusively due to the effect of adhesion. This particular example also explains the use of the term 'nominal point contact' [49].

By utilizing the JKR Eqs. (A.4) and (A.5), we transform Eq. (79) into the following equation with respect to the static contact radius a_0:

$$\frac{a_0^2}{R}\left(1 + \frac{4E^* a_0}{3k}\right) - \sqrt{\frac{2\pi w_0 a_0}{E^*}}\left(1 + \frac{2E^* a_0}{k}\right) = \frac{mg}{k}. \tag{80}$$

Let us introduce the notation

$$\mu = \frac{mg}{E^* R^2}. \tag{81}$$

Then, in view of (64), (66), and (81), we can rewrite Eq. (80) in the non-dimensionalized form as

$$\left(\frac{a_0}{R}\right)^2\left(\frac{4}{3}\frac{a_0}{R} + \kappa\right) - \frac{\sqrt{2}\chi_0^{3/2}}{3}\left(\frac{a_0}{R}\right)^{1/2}\left(\frac{2a_0}{R} + \kappa\right) = \mu. \tag{82}$$

The above equation predicts the relative initial contact radius a_0/R.

3.5.2. Steady-state vibrational nominal point contact

In view of (16), (17), and (78), Eq. (15) takes the form

$$\frac{a_{\mathrm{m}}^2}{R}\left(1 + \frac{4E^* a_{\mathrm{m}}}{3k}\right) - \sqrt{\frac{2\pi w_{\mathrm{eff}} a_{\mathrm{m}}}{E^*}}\left(1 + \frac{2E^* a_{\mathrm{m}}}{k}\right) = \frac{mg}{k}. \tag{83}$$

Evidently, Eq. (83) can be transformed to the form of Eq. (82) with respect to the ratio a_{m}/R, with the only difference that the dimensionless parameter χ_0 should now be replaced with the parameter χ_{eff} determined by formula (C.3). In light of (49), we have

$$\chi_{\mathrm{eff}} = \chi_0[\mathcal{J}_0(\bar{A})]^{2/3}. \tag{84}$$

Thus, the non-dimensionalized version of Eq. (83) takes the form

$$\left(\frac{a_{\mathrm{m}}}{R}\right)^2\left(\frac{4}{3}\frac{a_{\mathrm{m}}}{R} + \kappa\right) - \frac{\sqrt{2}\chi_0^{3/2}}{3}\mathcal{J}_0(\bar{A})\left(\frac{a_{\mathrm{m}}}{R}\right)^{1/2}\left(\frac{2a_{\mathrm{m}}}{R} + \kappa\right) = \mu. \tag{85}$$

Observe that in the Hertzian contact mechanics, *a priori* the ratio a_{m}/R is supposed to be small. That is why, it makes sense to non-dimensionalize the contact radius using the characteristic size of the JKR contact radius in the rigidly fixed nominal point contact, i.e., $a_{\circ} = (2\pi w_0 R^2/E^*)^{1/3}$. In this way, we introduce the non-dimensionalized variables

$$\bar{a}_{\mathrm{m}} = \frac{a_{\mathrm{m}}}{a_{\circ}}, \quad \bar{P}_{\mathrm{m}} = \frac{3RP_{\mathrm{m}}}{4E^* a_{\circ}^3}, \quad \bar{\delta}_{\mathrm{m}} = \frac{R\delta_{\mathrm{m}}}{a_{\circ}^2}, \tag{86}$$

where, in view of (64), we have $a_{\circ} = 2^{1/3}3^{-2/3}\chi_0 R$.

So, using Eq. $(86)_1$, we rewrite Eq. (85) as

$$\frac{2^{7/3}\chi_0}{3^{5/3}}\bar{a}_{\mathrm{m}}^3 + \kappa\bar{a}_{\mathrm{m}}^2 - \mathscr{J}_0(\bar{A})\left(\frac{2^{4/3}\chi_0}{3^{2/3}}\bar{a}_{\mathrm{m}}^{3/2} + \kappa\bar{a}_{\mathrm{m}}^{1/2}\right) = \frac{3^{4/3}\mu}{2^{2/3}\chi_0^2}. \tag{87}$$

For given values of the dimensionless parameters χ_0, κ, and μ, Eq. (87) can be solved numerically with respect to $\bar{a}_{\mathrm{m}}$ in terms of $\bar{A}$.

3.5.3. On passage through resonance

We consider the problem of vibroadhesion (37) for the linearized contact submodel based on relations (23) and (24)), which are further simplified as follows:

$$\tilde{P} \simeq \left(\frac{4E^*}{R}a_{\mathrm{m}}^2 - 3\sqrt{2\pi w_{\mathrm{eff}}E^* a_{\mathrm{m}}}\right)\tilde{a} + \sqrt{8\pi E^* a_{\mathrm{m}}^3}(\sqrt{w_{\mathrm{eff}}} - \sqrt{w}), \tag{88}$$

$$\tilde{\delta} \simeq \left(\frac{2a_{\mathrm{m}}}{R} - \sqrt{\frac{\pi w_{\mathrm{eff}}}{2E^* a_{\mathrm{m}}}}\right)\tilde{a} + \sqrt{\frac{2\pi a_{\mathrm{m}}}{E^*}}(\sqrt{w_{\mathrm{eff}}} - \sqrt{w}). \tag{89}$$

The application of the method of harmonic balance yields the same resulting Eq. (67), now rewritten in the form

$$\xi_{\mathrm{c}}^2 + \xi_{\mathrm{s}}^2 = \eta_1^2\left[(1-\bar{\omega}^2)^2 + 4\zeta^2\bar{\omega}^2\right], \tag{90}$$

with the same ξ_{c} and ξ_{s} (see Eqs. (41) and (42)), now represented as

$$\xi_{\mathrm{c}} = (1-\bar{\omega}^2)\check{\delta}_{\mathrm{c}} + 2\zeta\bar{\omega}\check{\delta}_{\mathrm{s}} + \check{P}_{\mathrm{c}}, \tag{91}$$

$$\xi_{\mathrm{s}} = (1-\bar{\omega}^2)\check{\delta}_{\mathrm{s}} - 2\zeta\bar{\omega}\check{\delta}_{\mathrm{c}} + \check{P}_{\mathrm{s}}, \tag{92}$$

where the dimensionless parameters $\check{\delta}_{\mathrm{c}}$, $\check{\delta}_{\mathrm{s}}$ and $\check{P}_{\mathrm{c}}$, $\check{P}_{\mathrm{s}}$ are obtained from $\tilde{\delta}_{\mathrm{c}}$, $\tilde{\delta}_{\mathrm{s}}$ and $\tilde{P}_{\mathrm{c}}$, $\tilde{P}_{\mathrm{s}}$ by dividing by R and kR, respectively, but with the asymptotically more accurate (than (32)–(35)) expressions for the harmonic coefficients $\tilde{\delta}_{\mathrm{c}}$, $\tilde{\delta}_{\mathrm{s}}$, $\tilde{P}_{\mathrm{c}}$, and $\tilde{P}_{\mathrm{s}}$, so that

$$\check{\delta}_{\mathrm{c}} = -\frac{2^{2/3}\chi_0^2}{3^{4/3}}\bar{a}_{\mathrm{m}}^{1/2}\mathscr{J}_{\mathrm{c}1}(\bar{A}), \tag{93}$$

$$\check{\delta}_{\mathrm{s}} = \frac{2^{4/3}\nu_0\chi_0}{3^{2/3}\bar{\omega}}\bar{A}\bar{a}_{\mathrm{m}}\left(1 - \frac{\mathscr{J}_1(\bar{A})}{4\bar{a}_{\mathrm{m}}^{3/2}}\right), \tag{94}$$

$$\check{P}_{\mathrm{c}} = -\frac{4\chi_0^3}{9\kappa}\bar{a}_{\mathrm{m}}^{3/2}\mathscr{J}_{\mathrm{c}1}(\bar{A}), \tag{95}$$

$$\check{P}_{\mathrm{s}} = \frac{2^{8/3}\nu_0\chi_0^2}{3^{4/3}\kappa\bar{\omega}}\bar{A}\bar{a}_{\mathrm{m}}^2\left(1 - \frac{3\mathscr{J}_1(\bar{A})}{4\bar{a}_{\mathrm{m}}^{3/2}}\right). \tag{96}$$

Here we have introduced the new dimensionless model parameter

$$\nu_0 = \frac{v_0}{\omega_0 R}. \tag{97}$$

The substitution of the non-dimensionalized expressions (91)–(96) into Eq. (90) leads to a single equation, which is algebraic with respect to $\bar{\omega}$ and transcendental with respect to $\bar{A}$. In conjunction with Eq. (87), it forms a system for evaluating the dimensionless parameters $\bar{a}_{\mathrm{m}}$ and $\bar{A}$, which (that is, the resulting system) is not limited to the case of vibrational nominal point contact.

Fig. 5 illustrates the variation of the dimensionless contact-radius oscillation amplitude A/a_{m} as a function of the dimensionless excitation angular velocity $\bar{\omega}$ for the following set of parameters: $\chi_0 = 2.589\times10^{-2}$, $\eta_1 = 3.883\times10^{-4}$, and $\nu_0 = 1.227\times10^{-5}$.

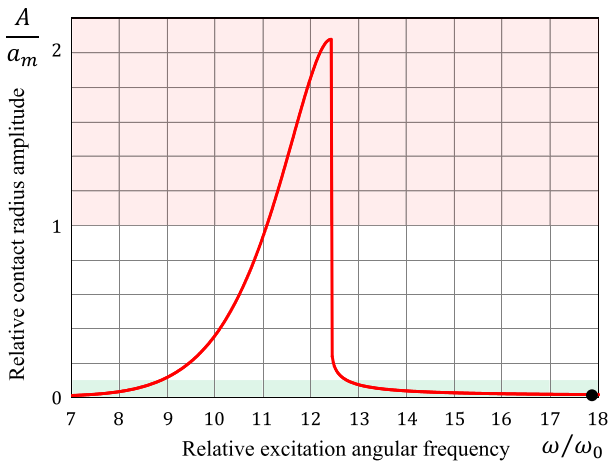

Fig. 5. Variation of the contact radius oscillation amplitude during passage through the system resonance. The dot symbol (in the right corner of the plot) indicates the position of the 200 Hz experiment for the case $h_1 = 20$ μm shown in Fig. 4.

According to (45), (86), and (97), we have

$$\frac{A}{a_{\mathrm{m}}} = \frac{3^{2/3}\nu_0\bar{A}}{2^{1/3}\chi_0\bar{a}_{\mathrm{m}}}. \tag{98}$$

Obviously, since the amplitude A of the contact-radius variation cannot exceed the contact-radius mean value a_{m}, the (upper) red-hatched area in Fig. 5 represents the geometrically impossible situation. Less obvious is to identify the region of applicability of the asymptotic model, as the latter assumes that $A \ll a_{\mathrm{m}}$ (see the (lower) green-hatched area in Fig. 5, which covers the region $A \le 0.1a_{\mathrm{m}}$). The plot presented in Fig. 5 has been drawn for the case $h_1 = 20$ μm. The choice of the excitation frequencies 200 Hz, 300 Hz, and 400 Hz (which corresponds to $\bar{\omega} = 17.85$, 26.78, and 35.7) falls within the region of the model applicability.

3.5.4. Nominal point contact of a rigidly fixed indenter

In the limit as k tends to infinity, Eqs. (79) and (80) respectively reduce to the equations $\delta_0 = 0$ and $a_0 = a_{\circ}$, so that $\bar{a}_{\mathrm{m}} = 1$ in quasi-static oscillations (see Eq. $(86)_1$). In addition, Eq. (87) simplifies as (cf. Eq. (56))

$$a_{\mathrm{m}} = \mathscr{J}_0^{2/3}(\bar{A}). \tag{99}$$

In view of (65), (66), (91), and (92), Eq. (90) reduces to the simple relation

$$\sqrt{\check{\delta}_{\mathrm{c}}^2 + \check{\delta}_{\mathrm{s}}^2} = \eta_1, \tag{100}$$

which states that the displacement oscillation amplitude is directly controlled by the rigid-base excitation amplitude.

The substitution of (93), (94) into Eq. (100) yields

$$\frac{2^{2/3}\chi_0^2}{3^{4/3}}\bar{a}_{\mathrm{m}}\mathscr{J}_{\mathrm{c}1}^2(\bar{A}) + \frac{\bar{A}^2\bar{a}_{\mathrm{m}}^2}{\check{\omega}^2}\left(1 - \frac{\mathscr{J}_1(\bar{A})}{4\bar{a}_{\mathrm{m}}^{3/2}}\right) = \bar{\eta}_1^2, \tag{101}$$

where we have introduced the notation

$$\bar{\eta}_1 = \frac{3^{4/3}\eta_1^2}{2^{2/3}\chi_0^2}. \tag{102}$$

We note that the right-hand sides of Eqs. (101) and (102) are equal to $h_1^2/a_{\circ}^2$.

Finally, the substitution of (99) into Eq. (101) results in a single equation with respect to the dimensionless internal variable $\bar{A}$.

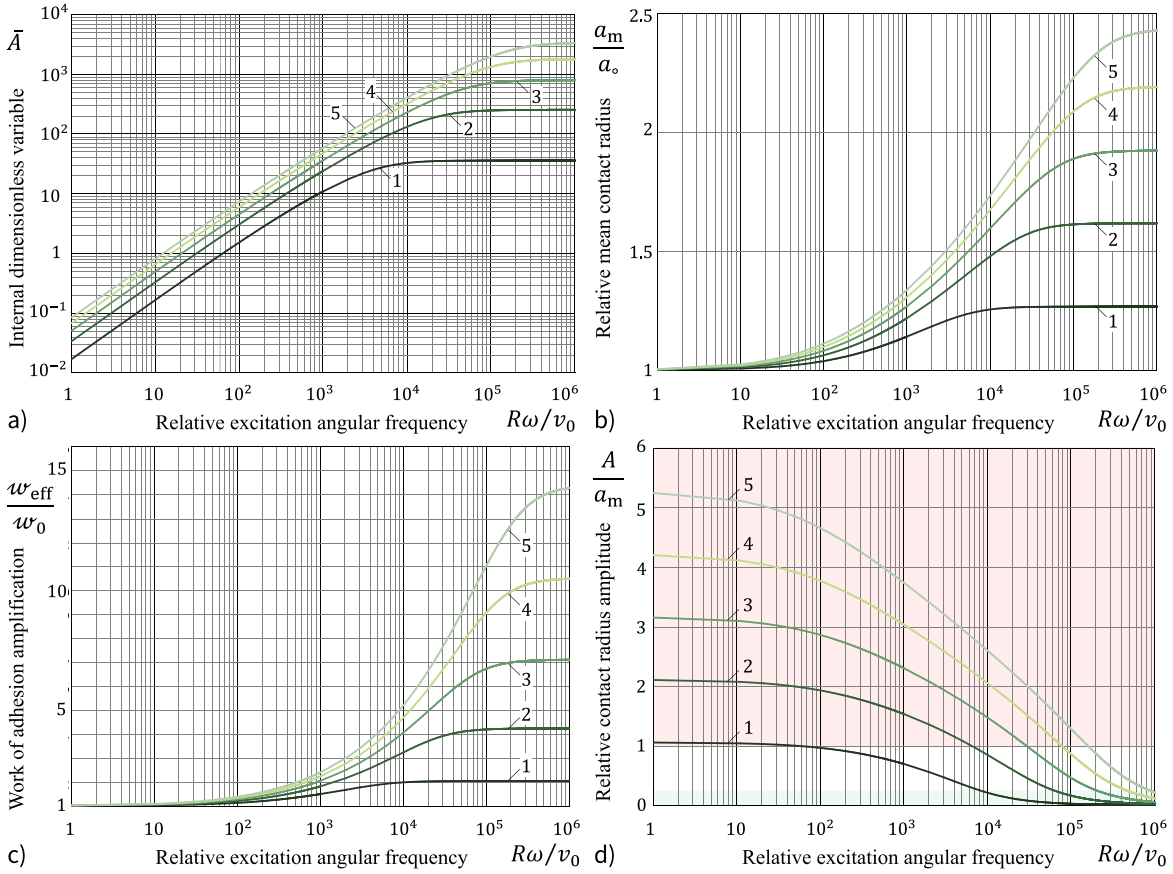

Fig. 6. Variation of the internal variable (a), relative mean contact radius (b), adhesive work amplification (c), and relative contact radius (d) in the case of nominal point contact for $\eta_1 = h_1/R$ corresponding to the five rigid-base excitation amplitudes $h_1 = 20, 40, 60, 80, 100$ μm with the indenter radius $R = 51.5$ mm shown in Fig. 4.

Fig. 6 illustrates the variation of the main parameters in the case of nominal point contact of a rigidly fixed hemispherical indenter for a specified value of the base excitation amplitude. The five chosen values of the dimensionless parameter $\bar{\eta}_1$ correspond to $h_1 = 20, 40, 60, 80, 100$ μm and $R = 51.5$ mm for $\chi_0 = 2.589 \times 10^{-2}$. This set of parameters is dictated by the experimental setup used in [35,48]. It should be emphasized that the interval of base excitation reported in [35,48] lies outside the range of $\breve{\omega}$ shown in Fig. 6. In other words, the leading-order asymptotic approximations are expected to provide robust predictions, as the frequency excitation effect diminishes for $\omega > 10^6(v_0/R)$.

3.6. Refined asymptotic model

Formulas (93)–(96), which are asymptotically more accurate than (47) and (48), can be utilized for refining the asymptotic approximations derived in Section 3.1. In particular, in the limit of high-frequency vibrations, from Eq. (90), in view of (91) and (92), it follows that

$$\sqrt{\breve{\delta}_c^2 + \breve{\delta}_s^2} = \eta_1, \tag{103}$$

or which is the same, $\tilde{\delta}_c^2 + \tilde{\delta}_s^2 = h_1^2$. The above relation means that at high frequency the rigid-base oscillation amplitude h_1 and the contact indentation amplitude $|\tilde{\delta}| = \sqrt{\tilde{\delta}_c^2 + \tilde{\delta}_s^2}$ are extremely close to each other. In the experiments reported in [35,48], the difference is just a few percent. We also note that in the leading asymptotic terms, Eq. (103) reduces to Eq. (44).

By setting $a_m = a_{cr}$ (see formulas (60) and (61)) in relations (93) and (94), we readily get

$$\breve{\delta}_c = -\frac{\chi_0^2}{3}\mathcal{J}_0^{1/3}\mathcal{J}_{c1}, \quad \breve{\delta}_s = \frac{\chi_0 \bar{A}_{cr}}{\breve{\omega}}\mathcal{J}_0^{2/3}\left(1 - \frac{\mathcal{J}_1}{3\mathcal{J}_0}\right), \tag{104}$$

where the integrals $\mathcal{J}_0$, $\mathcal{J}_1$, and $\mathcal{J}_{c1}$ are functions of the unknown critical value $\bar{A}_{cr}$ of the internal variable $\bar{A}$, and we have introduced the notation

$$\breve{\omega} = \frac{\omega}{v_0/R} = \frac{\bar{\omega}}{v_0}. \tag{105}$$

The substitution of (104) into Eq. (103) yields the equation

$$\frac{\chi_0^4}{9}\mathcal{J}_0^{2/3}(\bar{A})\mathcal{J}_{c1}^2(\bar{A}) + \frac{\chi_0^2}{\breve{\omega}^2}\bar{A}^2\mathcal{J}_0^{4/3}(\bar{A})\left(1 - \frac{\mathcal{J}_1(\bar{A})}{3\mathcal{J}_0(\bar{A})}\right)^2 = \eta_1^2 \tag{106}$$

that serves for evaluating the critical value $\bar{A}_{cr}$ as a function of the dimensionless excitation parameters $\breve{\omega}$ and η_1.

It can be easily checked that the second term on the left-hand side of Eq. (106) is not significant for the set of experimental data [35,48].

Fig. 7b shows the variation of the relative pull-off force predicted by the refined asymptotic model (106). As it is seen from Fig. 7a, the excitation frequency effect diminishes at high frequencies, which qualitatively agrees with the experimental findings [35,48].

Remark 3. It should be emphasized that Eq. (106) was derived from Eq. (103), which in turn has been obtained in the limit of high frequency vibrations. The dependence of the dimensionless excitation angular frequency $\breve{\omega}$ enters Eq. (106) from Eq. $(104)_2$. That is why,

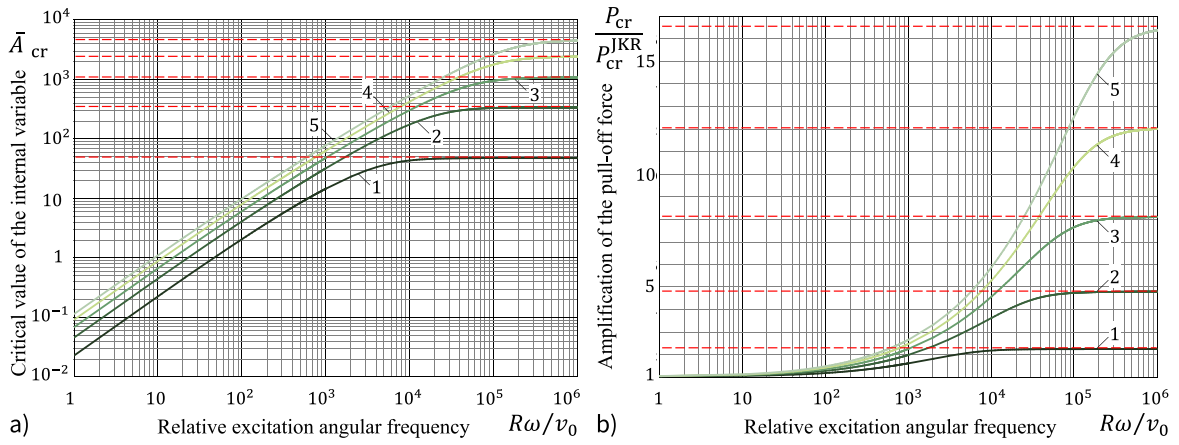

Fig. 7. The critical parameters, namely, the internal variable (a) and the pull-off force amplification (b) as functions of the normalized excitation angular velocity according to the refined asymptotic model (106). The dashed lines represent asymptotes for the corresponding curves at infinity.

the derivation of Eq. (103) from Eqs. (90)–(92) can be interpreted as ignoring the instrumental compliance effect.

3.7. Dynamic contact stiffness

According to the first harmonics balance, we have

$$\tilde{P} \simeq \tilde{P}_{\mathrm{c}} \cos \omega t' + \tilde{P}_{\mathrm{s}} \sin \omega t', \tag{107}$$

$$\tilde{\delta} \simeq \tilde{\delta}_{\mathrm{c}} \cos \omega t' + \tilde{\delta}_{\mathrm{s}} \sin \omega t', \tag{108}$$

and $\tilde{a} \simeq A \sin \omega t'$ (see formula $(25)_1$).

By using Euler's formula for complex numbers, we can represent the above relations in the complex form as

$$\tilde{P} = \mathrm{Re}\, \left\{ \tilde{P}_{\mathrm{A}} \exp(\mathrm{i}(\omega t' + \varphi_P)) \right\}, \tag{109}$$

$$\tilde{\delta} = \mathrm{Re}\, \left\{ \tilde{\delta}_{\mathrm{A}} \exp(\mathrm{i}(\omega t' - \varphi_{\delta})) \right\}, \tag{110}$$

where $\tilde{P}_{\mathrm{A}}$ and $\tilde{\delta}_{\mathrm{A}}$ are the force and indentation amplitudes, i.e.,

$$\tilde{P}_{\mathrm{A}} = \sqrt{\tilde{P}_{\mathrm{c}}^2 + \tilde{P}_{\mathrm{s}}^2}, \quad \tilde{\delta}_{\mathrm{A}} = \sqrt{\tilde{\delta}_{\mathrm{c}}^2 + \tilde{\delta}_{\mathrm{s}}^2}, \tag{111}$$

and we have introduced the phase angles φ_P and φ_{δ} as follows:

$$\cos \varphi_P = \tilde{P}_{\mathrm{c}}/\tilde{P}_{\mathrm{A}}, \quad \sin \varphi_P = -\tilde{P}_{\mathrm{s}}/\tilde{P}_{\mathrm{A}}, \tag{112}$$

$$\cos \varphi_{\delta} = \tilde{\delta}_{\mathrm{c}}/\tilde{\delta}_{\mathrm{A}}, \quad \sin \varphi_{\delta} = \tilde{\delta}_{\mathrm{s}}/\tilde{\delta}_{\mathrm{A}}. \tag{113}$$

Following Greenwood and Johnson [16] and in a direct analogy with the linear viscoelasticity, we introduce the complex contact stiffness, $\tilde{S}^*$, which is defined as the ratio of the complex oscillation force and the complex indentation from the curly braces in (109) and (110), that is

$$\tilde{S}^* = \frac{\tilde{P}_{\mathrm{A}}}{\tilde{\delta}_{\mathrm{A}}} \exp(\mathrm{i}(\varphi_P + \varphi_{\delta})). \tag{114}$$

The dynamic contact stiffness, $\tilde{S}$, is defined as the absolute modulus of the complex stiffness, i.e., $\tilde{S} = |\tilde{S}^*|$, and has the mechanical meaning of the ratio of the oscillation force and indentation amplitudes, that is

$$\tilde{S} = \frac{\tilde{P}_{\mathrm{A}}}{\tilde{\delta}_{\mathrm{A}}}. \tag{115}$$

By separating the real and imaginary parts, we can write

$$\tilde{S}^* = \tilde{S}' + \mathrm{i}\tilde{S}'', \tag{116}$$

where, in view of (111)–(114), we have

$$\tilde{S}' = \frac{\tilde{P}_{\mathrm{c}}\tilde{\delta}_{\mathrm{c}} + \tilde{P}_{\mathrm{s}}\tilde{\delta}_{\mathrm{s}}}{\tilde{\delta}_{\mathrm{c}}^2 + \tilde{\delta}_{\mathrm{s}}^2}, \quad \tilde{S}'' = \frac{\tilde{P}_{\mathrm{c}}\tilde{\delta}_{\mathrm{s}} - \tilde{P}_{\mathrm{s}}\tilde{\delta}_{\mathrm{c}}}{\tilde{\delta}_{\mathrm{c}}^2 + \tilde{\delta}_{\mathrm{s}}^2}. \tag{117}$$

The real quantities $\tilde{S}'$ and $\tilde{S}''$ may be called the storage and loss contact stiffnesses.

Let us rearrange formula $(117)_1$ as

$$\tilde{S}' = \frac{\tilde{P}_{\mathrm{c}}}{\tilde{\delta}_{\mathrm{c}}} \left(1 + \frac{\tilde{\delta}_{\mathrm{s}}^2}{\tilde{\delta}_{\mathrm{c}}^2}\right)^{-1} \left(1 + \frac{\tilde{P}_{\mathrm{s}}}{\tilde{P}_{\mathrm{c}}} \frac{\tilde{\delta}_{\mathrm{s}}}{\tilde{\delta}_{\mathrm{c}}}\right). \tag{118}$$

According to Eqs. (93)–(94), in view of (66), (97), (86), and (105), we have

$$\frac{\tilde{P}_{\mathrm{c}}}{\tilde{\delta}_{\mathrm{c}}} = 2E^* a_{\mathrm{m}}, \tag{119}$$

$$\frac{\tilde{\delta}_{\mathrm{s}}}{\tilde{\delta}_{\mathrm{c}}} = -\frac{6^{2/3} \bar{A} \bar{a}_{\mathrm{m}}^{1/2}}{\breve{\omega} \chi_0 \mathscr{J}_{\mathrm{c}1}(\bar{A})} \left(1 - \frac{\mathscr{J}_1(\bar{A})}{4\bar{a}_{\mathrm{m}}^{3/2}}\right), \tag{120}$$

$$\frac{\tilde{P}_{\mathrm{s}}}{\tilde{P}_{\mathrm{c}}} = -\frac{6^{2/3} \bar{A} \bar{a}_{\mathrm{m}}^{1/2}}{\breve{\omega} \chi_0 \mathscr{J}_{\mathrm{c}1}(\bar{A})} \left(1 - \frac{3\mathscr{J}_1(\bar{A})}{4\bar{a}_{\mathrm{m}}^{3/2}}\right). \tag{121}$$

In the limit of high-frequency oscillations, as $\breve{\omega}$ tends to infinity, formula (118) reduces to (119). In other words, at high frequency of the rigid-base excitation, the dynamic contact stiffness (we have $\tilde{S} \simeq \tilde{S}'$ as $\breve{\omega} \to \infty$) coincides with that for a cylindrical flat-ended punch, which is exactly the finding originally made by Greenwood and Johnson [16].

Observe that we have got two dimensionless excitation parameters η_1 and $\breve{\omega}$ that govern both internal parameters $\bar{a}_{\mathrm{m}}$ and $\bar{A}$. In the case of rigid fixation (corresponding to the problem setup in [16]), Eq. (103) applies and, in view of (93) and (94), we have

$$\frac{2^{4/3}\chi_0^4}{3^{8/3}} \bar{a}_{\mathrm{m}} \mathscr{J}_{\mathrm{c}1}^2(\bar{A}) + \frac{2^{8/3}\chi_0^2}{3^{4/3}\breve{\omega}^2} \bar{A}^2 \bar{a}_{\mathrm{m}}^2 \left(1 - \frac{\mathscr{J}_1(\bar{A})}{4\bar{a}_{\mathrm{m}}^{3/2}}\right)^2 = \eta_1^2. \tag{122}$$

In the case of nominal point contact for a rigidly fixed indenter, Eq. (87) (see also Eq. (83)) simplifies to the equation

$$\bar{a}_{\mathrm{m}}^{3/2} = \mathscr{J}_0(\bar{A}), \tag{123}$$

which reduces to the obvious relation $\bar{a}_{\mathrm{m}} = 1$ in the limit of small oscillation amplitude as $\bar{A}$ tends to zero, due to the adopted normalization $(86)_1$ and the limit property $\lim \mathscr{J}_0(\bar{A}) = 1$ as $\bar{A} \to 0$.

From Eq. (123), it follows that $\bar{a}_{\mathrm{m}} = \mathscr{J}_0^{2/3}(\bar{A})$, and the substitution of this expression into Eq. (122) allows us to derive a single equation for evaluating $\bar{A}$ in terms of η_1 and $\breve{\omega}$.

Fig. 8 shows the variation of the right-hand side of Eq. (118), with Eqs. (119)–(121), and (123) taken into account. In the limit as $\breve{\omega}$ tends to zero, formula (118) reduces to

$$\tilde{S}' \simeq 2E^* a_{\mathrm{m}} \left(1 - \frac{\mathscr{J}_1(\bar{A})}{4\bar{a}_{\mathrm{m}}^{3/2}}\right)^{-1} \left(1 - \frac{3\mathscr{J}_1(\bar{A})}{4\bar{a}_{\mathrm{m}}^{3/2}}\right),$$

which in the limit as $\bar{A} \to 0$ and $\bar{a}_{\mathrm{m}} \to 1$ exactly agrees with the formula for the mean incremental contact stiffness (C.2) applied for $a_{\mathrm{m}} = a_{\circ} = (2/9)^{1/3} \chi_0 R$, since $\mathscr{J}_0(0) = 1$ and $\mathscr{J}_1(0) = 1$.

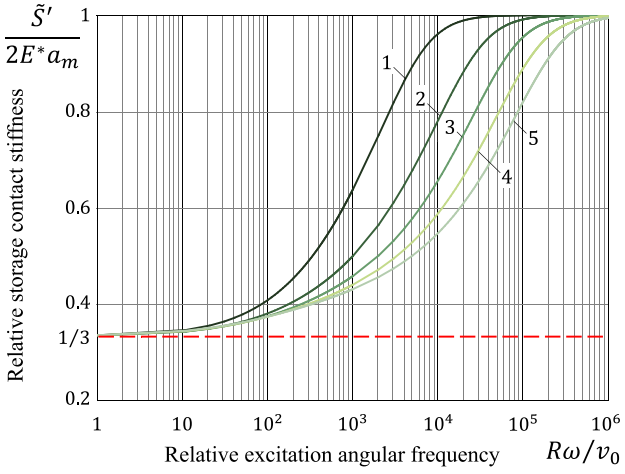

Fig. 8. Variation of the relative storage contact stiffness as a function of the relative excitation frequency $\tilde{\omega}$ for $\eta_1 = h_1/R$ corresponding to the five rigid-base excitation amplitudes $h_1 = 20, 40, 60, 80, 100$ μm with the indenter radius $R = 51.5$ mm.

Remark 4. In their seminal work [16], Greenwood and Johnson derived an elegant perturbation solution, called the approximate linear solution for the problem of oscillatory loading of the rate-dependent JKR-type normal contact, assuming the linear approximation

$$\frac{w}{w_0} = 1 - \frac{\dot{a}}{v_0}, \tag{124}$$

where $\dot{a} = \mathrm{d}a/\mathrm{d}t$ is the contact front velocity, and v_0 is some characteristic velocity. We recall that for shrinking contact (opening crack), we have $\dot{a} < 0$, and the right hand side of Eq. (124) is positive.

It is clear that the linear approximation (124) cannot be employed in the full range of loading rates, as for $\dot{a} > v_0$ formula (124) predicts negative values for the work of adhesion, which, of course, is not possible. That is why, Greenwood and Johnson assumed small variations of the contact radius a and the work of adhesion w from their respective equilibrium values a_0 and w_0. This, in particular, means that their application of formula (124) assumes that $|\dot{a}|/v_0 \ll 1$.

As a consequence of the equilibrium approximations, the Greenwood–Johnson model [16] is not capable to show the variation of the mean contact radius with the excitation frequency change. Overall, the equilibrium perturbation approach is not suitable for capturing the amplification of the work of adhesion which can be as high as an order of magnitude.

4. Discussion

First of all, strictly speaking the solution of the dynamic equilibrium problem (4), (5), and (8) in the case of harmonic excitation (11) is not periodic from the very beginning. This, in particular, means that the Bogoliubov averaging operator should be introduced in its general form

$$\underset{t}{M}\{u(t)\} = \lim_{T\to\infty} \frac{1}{T}\int_0^T u(t)\,\mathrm{d}t.$$

Since we are interested here in the steady state only, we simplified the analysis by adopting formula (14) that is applicable for periodic functions only.

By way of explanation, we note that Eqs. (4), (5), (16), and (17) can be equivalently recast in the linear decomposition form

$$\tilde{P} = \frac{4E^*}{3R}(a^3 - a_{\mathrm{m}}^3) + \sqrt{8\pi w_{\mathrm{eff}} E^*}\,(a_{\mathrm{m}}^{3/2} - a^{3/2}) + \sqrt{8\pi E^* a^3}\,(\sqrt{w_{\mathrm{eff}}} - \sqrt{w}), \tag{125}$$

$$\tilde{\delta} = \frac{a^2 - a_{\mathrm{m}}^2}{R} + \sqrt{\frac{2\pi w_{\mathrm{eff}}}{E^*}}\,(a_{\mathrm{m}}^{1/2} - a^{1/2}) + \sqrt{\frac{2\pi a}{E^*}}\,(\sqrt{w_{\mathrm{eff}}} - \sqrt{w}). \tag{126}$$

To simplify the asymptotic analysis (with the aim of extracting leading asymptotic terms), we first linearized the right-hand sides of Eqs. (125) and (126) with respect to $\tilde{a}$, thereby arriving to the asymptotic relations (23) and (24), and after that simplified the result further by making the linear terms (with respect to $\tilde{a}$) to be constant assuming that $w \simeq w_{\mathrm{eff}}$. This approach allowed us to derive approximations amendable for the qualitative analysis, however, perhaps, at the expense of accuracy of the quantitative analysis. That is why, if the numerical accuracy of the approximate solution is at stake, it is recommended to apply the method of harmonic balance to the indentation oscillation Eq. (20) with the exact JKR-type relations (125) and (126) taken into account. In such a case, Eqs. (43), (41), and (42) still apply but with $\tilde{P}_{\mathrm{c}}$, $\tilde{P}_{\mathrm{s}}$ and $\tilde{\delta}_{\mathrm{c}}$, $\tilde{\delta}_{\mathrm{s}}$ being evaluated from Eqs. (125) and (126).

The mechanical system under consideration (see Fig. 1) is a simplified representation of the experimental setup used in laboratory studies [48], where the resonance excitation regime is unsuitable for accurately measuring adhesive properties. The constructed leading-order asymptotic model is not applicable in the resonance case (as shown in Fig. 5), which requires a specialized averaging approach [42]. The primary condition for the asymptotic model's applicability is that the amplitude of the contact radius variation $\tilde{a}$ must be small compared to the mean contact radius a_{m}. This condition was satisfied in the experiments [48] (illustrated in Fig. 4) for relatively small values of the base excitation amplitude. It goes without saying that, in a quasi-linear dynamic system, the larger the excitation amplitude, the lower the accuracy of the results obtained using the averaging method.

Thus, the leading-order asymptotic model has a limited range of applicability (see Fig. 5), and its use is recommended only when the averaging method provides reasonably accurate and reliable predictions. The asymptotic simplifications of Eqs. (125) and (126) to Eqs. (23) and (24), respectively, have been identified as the primary cause for the reduced accuracy of the employed simplified variant of Bogoliubov's averaging method.

It should be noted that the quasi-static approximations for the pull-off force (see Sections 3.2 and 3.6) have two drawbacks. First, the adopted detachment criterion $a_{\mathrm{m}} = a_{\mathrm{cr}}$, with a_{cr} being dependent on w_{eff} according to the JKR model, does not account for the contact force oscillation during vibrational loading (see, e.g., [34]). Second, in real experiments, during detachment, the indenter has some pull-off velocity that compromises the quasi-static approximation $\dot{a}_{\mathrm{m}} \equiv 0$. Apparently, both neglected effects should be accounted for together, although the latter effect can be controlled independently, e.g., by making rigid-base excitation parameters h_0 and ω to be time-dependent.

Further, we note that the sample thickness H that enters Eqs. (1) and (A.1) does not appear in the analysis as it is hidden in the total length $\hat{h}$ of the disassembled elements. On the other side, the JKR Eqs. (A.4), (4) and (A.5), (5) simplify the tested sample's deformation response to that of an elastic half-space. Following [50], the JKR model can be extended to account for the sample thickness effect, and the closed-form forth-order asymptotic solution [51] is available for the case of moderately thin samples (when the contact diameter remains smaller than the sample thickness).

It is worth noting here that for $E = 2.8$ MPa, $\rho = 0.965\,\mathrm{g/cm^3}$, and $H = 2$ cm, the longitudinal waves can traverse the sample thickness approximately 27 times during a single oscillation period at a frequency of 200 Hz. This simple analysis justifies neglecting the dynamic waviness of the elastic sample, consistent with the Hertzian theory of impact.

Another way of generalizing the developed model lies in changing the indenter geometry from the Hertzian spherical (or, strictly speaking, paraboloidal) to the conical [52,53], monomial (i.e., power-law shaped) [54], spherical [55], or arbitrary convex shape [49]. This will concern the respective generalizations of the JKR model Eqs. (A.4), (4)

and (A.5), (5). Nevertheless, the general scheme of averaging remains the same.

Future studies could focus on a more detailed consideration of the physical and engineering aspects of the mechanical system under investigation. For instance, the linear reaction equation for the fixation element (see Eq. (2)) could be replaced with a nonlinear hereditary model [56] or modeled via a fractional-derivative approach [57]. The inertial properties of the elastic sample could be approximately incorporated in a usual way by introducing an additional degree of freedom into the dynamic system. Additionally, the assumption of displacement-controlled excitation could be replaced with a more realistic model that accounts for the finite power of the excitation motor. While these generalizations would complicate the dynamic system, our key findings regarding the asymptotic modeling of effective work of adhesion would remain valid, provided that the rate-dependent adhesion phenomenon can be accurately described by the Gent–Schultz law with sufficient precision for practical applications.

5. Conclusion

A leading-order asymptotic model of vibroadhesion has been developed using Bogoliubov's averaging approach in conjunction with the method of harmonic balance. The assumption of small-amplitude, high-frequency vibrations of the exciting rigid base allowed to greatly simplify the resulting asymptotic relations. The effective work of adhesion is defined in implicit form, since the mean contact radius and the contact radius oscillation amplitude need to be determined in terms of the rigid-base excitation parameters. The quasi-static estimate for the pull-off force shows a reasonably good agreement with experimental data available in the literature.

CRediT authorship contribution statement

I. Argatov: Writing – review & editing, Writing – original draft, Visualization, Validation, Methodology, Investigation, Formal analysis, Data curation, Conceptualization. **A. Papangelo:** Writing – review & editing, Writing – original draft, Supervision, Project administration, Investigation, Funding acquisition, Conceptualization. **M. Ciavarella:** Writing – review & editing, Writing – original draft, Supervision, Formal analysis, Conceptualization.

Acknowledgments

We thank Dr. Michele Tricarico for useful discussions of the experimental results. The main results have been presented at the Departmental Research Seminar, Department of Mechanics Mathematics and Management, Politecnico di Bari. We are grateful to Prof. Giuseppe Carbone for valuable discussion and comments. The authors were partly supported by the Italian Ministry of University and Research under the Programme "Department of Excellence" Legge 232/2016 (Grant No. CUP – D93C23000100001). A.P. was supported by the European Union (ERC-2021-STG, "Towards Future Interfaces With Tuneable Adhesion By Dynamic Excitation" – SURFACE, Project ID: 101039198, CUP: D95F22000430006). Views and opinions expressed are however those of the authors only and do not necessarily reflect those of the European Union or the European Research Council. Neither the European Union nor the granting authority can be held responsible for them.

Declaration of competing interest

The authors declare that they have no known competing financial interests or personal relationships that could have appeared to influence the work reported in this paper.

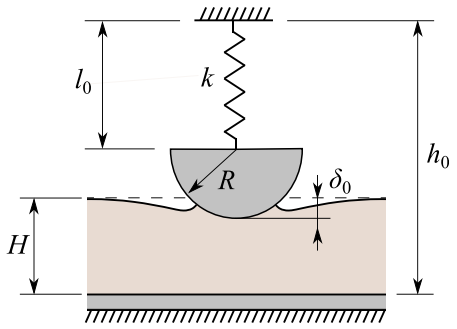

Fig. 9. Schematic of the adhesive contact between a hemispherical probe and an elastic sample: Static equilibrium.

Appendix A. Static equilibrium

We consider normal indentation of an elastic sample of finite thickness, H, performed with a hemispherical indenter of radius, R, and mass, m. It is assumed that the indenter is connected to a force sensor via a linear spring of stiffness, k, and some undeformed length, $\hat{l}$, whereas the tested sample is firmly attached to a rigid base through which a small-amplitude, high-frequency, displacement-controlled vibration stimulus can be applied.

So, in a static assembly, when the indenter maintains an adhesive contact with the sample surface (see Fig. 9), the total length of the assembly, h_0, can be calculated as

$$h_0 = l_0 + R + (H - \delta_0), \tag{A.1}$$

where δ_0 is the indenter displacement which characterizes the level of indentation, and l_0 is the length of the deformed spring which defines the spring elongation

$$x_s = l_0 - \hat{l}. \tag{A.2}$$

Let F_0 denote the spring reaction such that

$$F_0 = kx_s. \tag{A.3}$$

For describing the static adhesive contact between the rigid spherical indenter and the compliant elastic sample we apply the JKR theory stating that the indenter displacement δ_0 and the contact force P_0 are related via the contact radius a_0 as

$$P_0 = \frac{4E^*a_0^3}{3R} - \sqrt{8\pi w_0 E^* a_0^3}, \tag{A.4}$$

$$\delta_0 = \frac{a_0^2}{R} - \sqrt{\frac{2\pi w_0 a_0}{E^*}}, \tag{A.5}$$

where $E^* = E/(1-\nu^2)$ is the reduced elastic modulus, E and ν are Young's modulus and Poisson's ratio of the sample material, and w_0 is the thermodynamic (equilibrium) work of adhesion (we have changed the notation $\Delta\gamma$ for consistency with the case of rate-dependent adhesion). It is to note here that the classical Johnson–Kendall–Roberts (JKR) theory [58] does not account for the sample thickness H, assuming that $a_0 \ll H$ as well as $a_0 \ll R$.

The equation of static equilibrium of the indenter implies that

$$F_0 + P_0 = mg, \tag{A.6}$$

where g is the gravitational acceleration.

Hence, in view of (A.2), (A.3), and (A.6), Eq. (A.1) can be rewritten as

$$h_0 = \hat{h} + \frac{mg}{k} - \frac{P_0}{k} - \delta_0, \tag{A.7}$$

where we have introduced the total length of the disassembled system elements (spring, indenter, and sample)

$$\hat{h} = \hat{l} + R + H. \tag{A.8}$$

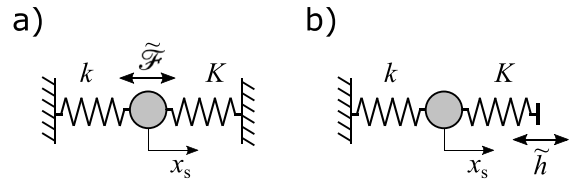

Fig. 10. Simple schematics of (a) load-excitation and (b) base-excitation experimental setups.

Thus, the problem of static equilibrium is formed by three Eqs. (A.4), (A.5), and (A.7) which contain three unknowns a_0, P_0, and δ_0, since both geometrical parameters $\hat{h}$ and h_0 are supposed to be known. Indeed, while $\hat{h}$ is determined by the geometry of the disassembled system alone, h_0 controls the level of loading (compressive for $h_0 < \hat{h}$ or tensile for $h_0 > \hat{h}$).

Appendix B. Load- and base-excitation experimental setups

Let us come back to Eq. (20) and consider (for simplicity of presentation) the non-dissipative case, when $c = 0$, in the situation of fixation-element resonance excitation, when $\omega = \sqrt{k/m}$. In such a case, Eq. (20) reduces to the homogeneous differential equation $m\ddot{\tilde{\delta}} + k\tilde{\delta} + \tilde{P} = 0$, because the forcing term $\tilde{\mathscr{F}}$ disappears (see formula (20) among others). On the contrary, nothing similar happens with Eq. (13), whose oscillation part takes the form $m\ddot{\tilde{\delta}} + k\tilde{\delta} + \tilde{P} = \tilde{\mathscr{F}}$ with $\tilde{\mathscr{F}} = \mathscr{F}_1 \sin\omega t$. This paradoxical situation can be explained as follows.

We consider two linear one-degree-of-freedom non-dissipative systems (see Fig. 10). In the first case (see Fig. 10a), the model equation is as simple as $m\ddot{x}_s + (k+K)x_s = \mathscr{F}_1 \sin\omega t$. In the second case, the model equation can be written as $m\ddot{x}_s + kx_s + \tilde{P} = 0$, where $\tilde{P} = K\delta$ and $\delta = x_s - \tilde{h}$ with $\tilde{h} = h_1 \sin\omega t$ (see Eqs. (3), (7), and $(21)_2$ applied for $\hat{h} = h_0$).

Hence, in the second case (see Fig. 10b), we can represent the model equation in the following two forms:

$$m\ddot{x}_s + (k+K)x_s = Kh_1 \sin\omega t, \tag{B.1}$$

$$m\ddot{\delta} + (k+K)\delta = (m\omega^2 - k)h_1 \sin\omega t. \tag{B.2}$$

It is of interest to look at the solution of Eq. (B.1) in the special case when $\omega = \sqrt{k/m}$ and the right-hand side of Eq. (B.2) vanishes. Since this type of excitation is not resonant for Eq. (B.1), we easily find that $x_s = [Kh_1/(k+K-m\omega^2)]\sin\omega t$. This result immediately implies that

$$\delta = x_s - h_1 \sin\omega t = -\frac{h_1(k-m\omega^2)}{k+K-m\omega^2}\sin\omega t. \tag{B.3}$$

From here, we readily see that $\delta \equiv 0$ in the special case under consideration (i.e., $\omega = \sqrt{k/m}$), meaning that the K-spring remains undeformed if the second dynamic system (see Fig. 10b) is excited at the resonance frequency of the k-spring.

Appendix C. Incremental contact stiffness

Based on the asymptotic formulas (88) and (89), now, expressing $\tilde{a}$ in terms of $\tilde{\delta}$ (by using Eq. (89)) and substituting the obtained result into Eq. (88), we can write

$$\tilde{P} \simeq S_{\mathrm{m}}^{\mathrm{eff}}\tilde{\delta} + \sqrt{8\pi E^* a_{\mathrm{m}}^3}(\sqrt{w} - \sqrt{w_{\mathrm{eff}}})\left(\frac{S_{\mathrm{m}}^{\mathrm{eff}}}{2E^* a_{\mathrm{m}}} - 1\right), \tag{C.1}$$

where $S_{\mathrm{m}}^{\mathrm{eff}}$ is the mean incremental contact stiffness of the effective JKR adhesive contact of radius a_{m}, that is

$$S_{\mathrm{m}}^{\mathrm{eff}} = 2E^* a_{\mathrm{m}}\left(1 - \frac{\chi_{\mathrm{eff}}^{3/2}}{6\sqrt{2}}\left(\frac{R}{a_{\mathrm{m}}}\right)^{3/2}\right)^{-1}\left(1 - \frac{\chi_{\mathrm{eff}}^{3/2}}{2\sqrt{2}}\left(\frac{R}{a_{\mathrm{m}}}\right)^{3/2}\right), \tag{C.2}$$

and we have introduced the notation

$$\chi_{\mathrm{eff}} = \left(\frac{9\pi w_{\mathrm{eff}}}{E^* R}\right)^{1/3}. \tag{C.3}$$

In view of (60), (C.2), and (C.3), it can be verified that $S_{\mathrm{m}}^{\mathrm{eff}} = 0$ for $a_{\mathrm{m}} = a_{\mathrm{c}}$, where a_{c} is the JKR critical value determined by the relation $\mathrm{d}P_{\mathrm{m}}/\mathrm{d}a_{\mathrm{m}} = 0$ according to Eq. (16). In other words, the mean contact stiffness of the tested sample at the detachment vanishes, if the detachment event is determined by the maximum of the mean contact force. This, in particular, *a priori* means that in order to minimize the instrumental effect, the system should be excited far from the resonance of the fixation subsystem comprised of the hemispherical indenter and the fixation element.

Further, in light of (47) and (48), we have

$$\tilde{\delta} \simeq \tilde{\delta}_{\mathrm{c}} \cos\omega t', \quad \tilde{P} \simeq \tilde{P}_{\mathrm{c}} \cos\omega t'. \tag{C.4}$$

Thus, in the leading asymptotic terms, the high-frequency assumption (see Eq. (44)) implies that the indenter oscillation amplitude $|\tilde{\delta}_{\mathrm{c}}|$ is determined by the base excitation amplitude h_1.

Moreover, from Eqs. (47) and (48), it follows that

$$\frac{\tilde{P}_{\mathrm{c}}}{\tilde{\delta}_{\mathrm{c}}} = 2E^* a_{\mathrm{m}}, \tag{C.5}$$

where the right-hand side coincides with the incremental stiffness of circular frictionless non-adhesive contact. Still, the effect of rate-dependent adhesion is taken into account via the mean contact radius a_{m} that depends on the relative contact radius oscillation amplitude $\bar{A}$ (see Eqs. (16), (17), and (49) among others).

On the other hand, we recall that the incremental contact stiffness can be evaluated as

$$S = \frac{\mathrm{d}P}{\mathrm{d}\delta} = \frac{\mathrm{d}P/\mathrm{d}t}{\mathrm{d}\delta/\mathrm{d}t}. \tag{C.6}$$

Hence, in view of Eqs. (12), under the assumption that P_{m} and δ_{m} are constants, from (C.4) and (C.6), it formally follows that $S \simeq \tilde{P}_{\mathrm{c}}/\tilde{\delta}_{\mathrm{c}}$.

Thus, in light of Eqs. (88) and (89), it can be seen that the simple paradoxical result $S \simeq 2E^* a_{\mathrm{m}}$ (which enters into contradiction with the asymptotic approximation (C.2) for the effective incremental contact stiffness $S_{\mathrm{m}}^{\mathrm{eff}}$) was obtained by neglecting the quasi-static contribution that comes from the first terms on the right-hand sides of Eqs. (23) and (24) (see also Eq. (46) which simplifies to $\tilde{\delta}_{\mathrm{s}} = 0$). This consideration prompts the construction of a refined asymptotic model that, in particular, accounts for the underlined term neglected in (46), but this is already a different story. Nevertheless, as it was shown in Section 3.7, the asymptotic formula (C.5) reconciles with the high-frequency asymptotics of the storage dynamic stiffness.

Data availability

No data was used for the research described in the article.

References

[1] B.V. Deryagin, N.A. Krotova, V.P. Smilga, Adhesion of solids, Consultants Bureau, New York, 1978.
[2] K. Kendall, Molecular Adhesion and Its Applications: The Sticky Universe, Kluwer Academic/Plenum Publishers, New York, 2001.
[3] D. Maugis, Contact, Adhesion and Rupture of Elastic Solids, Springer-Verlag, Berlin, 2000.
[4] J.R. Barber, Contact Mechanics, Springer, Cham, Switzerland, 2018.
[5] B.V. Derjaguin, N.V. Churaev, V.M. Muller, Surface Forces, Springer-Verlag, Boston, 1987.
[6] F.M. Borodich, The Hertz-type and adhesive contact problems for depth-sensing indentation, Adv. Appl. Mech. 47 (2014) 225–366.
[7] M. Ciavarella, J. Joe, A. Papangelo, J. Barber, The role of adhesion in contact mechanics, J. R. Soc. Interface 16 (151) (2019) 20180738.
[8] P.R. Guduru, C. Bull, Detachment of a rigid solid from an elastic wavy surface: Experiments, J. Mech. Phys. Solids 55 (3) (2007) 473–488.

[9] A. Papangelo, M. Ciavarella, A numerical study on roughness-induced adhesion enhancement in a sphere with an axisymmetric sinusoidal waviness using Lennard–Jones interaction law, Lubricants 8 (9) (2020) 90.
[10] H. Gao, H. Yao, Shape insensitive optimal adhesion of nanoscale fibrillar structures, Proc. Natl. Acad. Sci. 101 (21) (2004) 7851–7856.
[11] I.I. Argatov, Controlling the adhesive pull-off force via the change of contact geometry, Phil. Trans. R. Soc. A 379 (2203) (2021) 20200392.
[12] A.N. Gent, J. Schultz, Effect of wetting liquids on the strength of adhesion of viscoelastic material, J. Adhes. 3 (4) (1972) 281–294.
[13] D. Maugis, M. Barquins, Fracture mechanics and adherence of viscoelastic solids, in: L.H. Lee (Ed.), Adhesion and Adsorption of Polymers, Plenum Press, New York, 1980, pp. 203–277.
[14] V.M. Muller, On the theory of pull-off of a viscoelastic sphere from a flat surface, J. Adhes. Sci. Technol. 13 (9) (1999) 999–1016.
[15] M. Ciavarella, Improved muller approximate solution of the pull-off of a sphere from a viscoelastic substrate, J. Adhes. Sci. Technol. 35 (20) (2021) 2175–2183.
[16] J.A. Greenwood, K.L. Johnson, Oscillatory loading of a viscoelastic adhesive contact, J. Colloid Interface Sci. 296 (1) (2006) 284–291.
[17] A. Papangelo, M. Ciavarella, Detachment of a rigid flat punch from a viscoelastic material, Tribol. Lett. 71 (2) (2023) 48.
[18] I.I. Argatov, I.A. Lyashenko, V.L. Popov, Rate-dependent JKR-type decohesion of a cylindrical punch from an elastic substrate, Phys. Scr. 98 (5) (2023) 055905.
[19] R.A. Schapery, On the mechanics of crack closing and bonding in linear viscoelastic media, Int. J. Fract. 39 (1989) 163–189.
[20] J. Greenwood, The theory of viscoelastic crack propagation and healing, J. Phys. D: Appl. Phys. 37 (18) (2004) 2557.
[21] B.N.J. Persson, E.A. Brener, Crack propagation in viscoelastic solids, Phys. Rev. E 71 (3) (2005) 036123.
[22] K. Wahl, S. Asif, J. Greenwood, K. Johnson, Oscillating adhesive contacts between micron-scale tips and compliant polymers, J. Colloid Interface Sci. 296 (1) (2006) 178–188.
[23] A. Maghami, Q. Wang, M. Tricarico, M. Ciavarella, Q. Li, A. Papangelo, Bulk and fracture process zone contribution to the rate-dependent adhesion amplification in viscoelastic broad-band materials, J. Mech. Phys. Solids 193 (2024) 105844.
[24] I.I. Argatov, I.A. Lyashenko, V.L. Popov, Ad hoc modeling of rate-dependent adhesion in indentation relaxation testing, Materials 17 (16) (2024) 3944.
[25] L. Shui, L. Jia, H. Li, J. Guo, Z. Guo, Y. Liu, Z. Liu, X. Chen, Rapid and continuous regulating adhesion strength by mechanical micro-vibration, Nat. Commun. 11 (1) (2020) 1583.
[26] G. Giordano, R.B.N. Scharff, M. Carlotti, M. Gagliardi, C. Filippeschi, A. Mondini, A. Papangelo, B. Mazzolai, Mechanochromic suction cups for local stress detection in soft robotics, Adv. Intell. Syst. (2024) 2400254.
[27] J. Yi, W. Haouas, M. Gauthier, K. Rabenorosoa, A PDMS/Silicon adhesion control method at millimeter-scale based on microvibration, Adv. Intell. Syst. (2024) 2400394.
[28] Y. Fang, X. Tan, A dynamic JKR model with application to vibrational release in micromanipulation, in: 2006 IEEE/RSJ International Conference on Intelligent Robots and Systems, IEEE, 2006, pp. 1341–1346.
[29] O. Sirin, M. Ayyildiz, B.N.J. Persson, C. Basdogan, Electroadhesion with application to touchscreens, Soft Matter 15 (8) (2019) 1758–1775.
[30] I.I. Argatov, F.M. Borodich, A macro model for electroadhesive contact of a soft finger with a touchscreen, IEEE Trans. Haptics 13 (3) (2020) 504–510.
[31] A. Papangelo, R. Lovino, M. Ciavarella, Electroadhesive sphere-flat contact problem: A comparison between DMT and full iterative finite element solutions, Tribol. Int. 152 (2020) 106542.
[32] I.I. Blekhman, Vibrational dynamic materials and composites, J. Sound Vib. 317 (3–5) (2008) 657–663.
[33] I.I. Blekhman, Vibrational Mechanics: Nonlinear Dynamic Effects, General Approach, Applications, World Scientific, Singapore, 2000.
[34] C. Mandriota, N. Menga, G. Carbone, Enhancement of adhesion strength in viscoelastic unsteady contacts, J. Mech. Phys. Solids 192 (2024) 105826.
[35] M. Ciavarella, M. Tricarico, A. Papangelo, On the dynamic JKR adhesion problem, Mech. Mater. (2025) 105252.
[36] S. Muthukumar, R. DesRoches, A hertz contact model with non-linear damping for pounding simulation, Earthq. Eng. Struct. Dyn. 35 (7) (2006) 811–828.
[37] W. Serweta, A. Okolewski, B. Blazejczyk-Okolewska, K. Czolczynski, T. Kapitaniak, Lyapunov exponents of impact oscillators with Hertz's and Newton's contact models, Int. J. Mech. Sci. 89 (2014) 194–206.
[38] W. Lacarbonara, F. Vestroni, Nonclassical responses of oscillators with hysteresis, Nonlinear Dynam. 32 (2003) 235–258.
[39] F. Vestroni, P. Casini, Nonlinear dynamics and phenomena in oscillators with hysteresis, in: Modern Trends in Structural and Solid Mechanics 2: Vibrations, John Wiley & Sons, Ltd, 2021, pp. 185–202.
[40] I. Argatov, L. Voll, V.L. Popov, A hysteretic model of localized frictional contacts with instrumental stiffness, Meccanica 57 (8) (2022) 1783–1799.
[41] N.N. Bogoliubov, Theory of perturbations in nonlinear mechanics, in: Institute for Structural Mechanics, UkrSSR Academy of Sciences, Collection of Papers, (14) 1950, pp. 9–34.
[42] N.N. Bogoliubov, Y.A. Mitropolsky, Asymptotic methods in the theory of non-linear oscillations, Gordon and Breach, New York, 1961.
[43] I.A. Mitropolsky, Averaging method in non-linear mechanics, Int. J. Non-Linear Mech. 2 (1) (1967) 69–96.
[44] R. Masiani, D. Capecchi, F. Vestroni, Resonant and coupled response of hysteretic two-degree-of-freedom systems using harmonic balance method, Int. J. Non-Linear Mech. 37 (8) (2002) 1421–1434.
[45] R. Genesio, A. Tesi, Harmonic balance methods for the analysis of chaotic dynamics in nonlinear systems, Automatica 28 (3) (1992) 531–548.
[46] N.M. Krylov, N.N. Bogoliubov, Introduction to Nonlinear Mechanics, Princeton University Press, Princeton, 1949.
[47] G. Carbone, C. Mandriota, N. Menga, Theory of viscoelastic adhesion and friction, Extrem. Mech. Lett. 56 (2022) 101877.
[48] M. Tricarico, M. Ciavarella, A. Papangelo, Enhancement of adhesion strength through microvibrations: modeling and experiments, J. Mech. Phys. Solids (2025) 106020.
[49] I.I. Argatov, I.A. Lyashenko, V.L. Popov, Adhesive sliding with a nominal point contact: Postpredictive analysis, Internat. J. Engrg. Sci. 200 (2024) 104055.
[50] A.J. Crosby, K.R. Shull, Adhesive failure analysis of pressure-sensitive adhesives, J. Polym. Sci. Part B: Polym. Phys. 37 (24) (1999) 3455–3472.
[51] I.I. Argatov, F.M. Borodich, V.L. Popov, JKR adhesive contact for a transversely isotropic layer of finite thickness, J. Phys. D: Appl. Phys. 49 (4) (2015) 045307.
[52] M. Ciavarella, Pull-off of a rigid cone from a viscoelastic substrate, J. Adhes. Sci. Technol. 38 (14) (2024) 2647–2658.
[53] S.-W. Chen, X.-M. Liang, G.-F. Wang, Influence of adhesion on oscillatory indentations of viscoelastic biomaterials by a rigid cone, J. Phys. D: Appl. Phys. 57 (31) (2024) 315401.
[54] F.M. Borodich, B.A. Galanov, M.M. Suarez-Alvarez, The JKR-type adhesive contact problems for power-law shaped axisymmetric punches, J. Mech. Phys. Solids 68 (2014) 14–32.
[55] I.I. Argatov, F.J. Sabina, Asymptotic analysis of the substrate effect for an arbitrary indenter, Q. J. Mech. Appl. Math. 66 (1) (2013) 75–95.
[56] K. Hedrih, Energy analysis in a nonlinear hybrid system containing linear and nonlinear subsystems coupled by hereditary element, Nonlinear Dynam. 51 (2008) 127–140.
[57] Y.A. Rossikhin, M. Shitikova, Analysis of nonlinear vibrations of a two-degree-of-freedom mechanical system with damping modelled by a fractional derivative, J. Engrg. Math. 37 (4) (2000) 343–362.
[58] K.L. Johnson, K. Kendall, A.D. Roberts, Surface energy and the contact of elastic solids, Proc. R. Soc. Lond. A 324 (1558) (1971) 301–313.